Monthly Notices of the ROYAL ASTRONOMICAL SOCIETY

Mon. Not. R. Astron. Soc. **426,** 296–316 (2012) doi:10.1111/j.1365-2966.2012.21705.x

Compact groups of galaxies selected by stellar mass: the 2MASS compact group catalogue

Eugenia Díaz-Giménez,[1,2,3]★ Gary A. Mamon,[4] Marcela Pacheco,[1] Claudia Mendes de Oliveira[3] and M. Victoria Alonso[1,2]

[1]*Instituto de Astronomía Teórica y Experimental, IATE, CONICET, Argentina*
[2]*Observatorio Astronómico, Universidad Nacional de Córdoba, Laprida 854, X5000BGR, Córdoba, Argentina*
[3]*Instituto de Astronomia, Geofisica e Ciencias Atmosfericas, IAG, USP, Rua do Matão 1226, São Paulo, Brazil*
[4]*Institut d'Astrophysique de Paris (UMR 7095: CNRS & UPMC), 98 bis Bd Arago, F-75014 Paris, France*

Accepted 2012 July 11. Received 2012 July 9; in original form 2012 April 6

ABSTRACT

We present a photometric catalogue of compact groups of galaxies (*p2MCG*s) automatically extracted from the Two-Micron All Sky Survey (2MASS) extended source catalogue. A total of 262 *p2MCG*s are identified, following the criteria defined by Hickson, of which 230 survive visual inspection (given occasional galaxy fragmentation and blends in the 2MASS parent catalogue). Only one quarter of these 230 groups were previously known compact groups (CGs). Among the 144 *p2MCG*s that have all their galaxies with known redshifts, 85 (59 per cent) have four or more accordant galaxies. This *v2MCG* sample of velocity-filtered *p2MCG*s constitutes the largest sample of CGs (with $N \geq 4$) catalogued to date, with both well-defined selection criteria and velocity filtering, and is the first CG sample selected by stellar mass. It is fairly complete up to $K_{\rm group} \sim 9$ and radial velocity of $\sim$6000 km s^{-1}.

We compared the properties of the 78 *v2MCG*s with median velocities greater than 3000 km s^{-1} with the properties of other CG samples, as well as those (*mvCG*s) extracted from the semi-analytical model (SAM) of Guo et al. run on the high-resolution Millennium-II simulation. This *mvCG* sample is similar (i.e. with 2/3 of physically dense CGs) to those we had previously extracted on three other SAMs run on the Millennium simulation with 125 times worse spatial and mass resolutions. The space density of *v2MCG*s within 6000 km s^{-1} is $8.0 \times 10^{-5}\, h^3$ Mpc^{-3}, i.e. four times that of the Hickson sample [Hickson Compact Group (HCG)] up to the same distance and with the same criteria used in this work, but still 40 per cent less than that of *mvCG*s.

The *v2MCG* constitutes the first group catalogue to show a statistically large first–second ranked galaxy magnitude gap according to Tremaine–Richstone statistics, as expected if the first ranked group members tend to be the products of galaxy mergers, and as confirmed in the *mvCG*s. The *v2MCG* is also the first observed sample to show that first-ranked galaxies tend to be centrally located, again consistent with the predictions obtained from *mvCG*s. We found no significant correlation of group apparent elongation and velocity dispersion in the quartets among the *v2MCG*s, and the velocity dispersions of apparently round quartets are not significantly larger than those of chain-like ones, in contrast to what has been previously reported in HCGs.

By virtue of its automatic selection with the popular Hickson criteria, its size, its selection on stellar mass, and its statistical signs of mergers and centrally located brightest galaxies, the *v2MCG* catalogue appears to be the laboratory of choice to study physically dense groups of four or more galaxies of comparable luminosity.

Key words: catalogues – galaxies: groups: general – galaxies: interactions.

★E-mail: eugeniadiazz@gmail.com

1 INTRODUCTION

Compact groups (CGs) of at least four galaxies of comparable luminosity are the densest galaxy associations known at present. The compactness of these groups is so high that the typical projected separations between galaxies are of the order of their own diameters (Hickson et al. 1992; Focardi & Kelm 2002), hence their space densities can exceed those of the cores of rich clusters. The combination of their very high number densities and low velocity dispersion makes CGs the ideal site of galaxy mergers (Mamon 1992, see also Carnevali, Cavaliere & Santangelo 1981; Barnes 1985; Mamon 1987a; Bode, Cohn & Lugger 1993).

Since the discovery of Stephan's quintet (Stephan 1877) and Seyfert's Sextet (Seyfert 1948), several surveys of CGs have been undertaken: Rose (1977) and Hickson (1982) performed visual identifications of CGs on the Palomar Observatory Sky Survey (POSS) I photographic plates. Thereafter, the new catalogues of CGs used automatic searches: from the COSMOS/United Kingdom Schmidt Telescope (UKST) Southern Galaxy Catalogue (Prandoni, Iovino & MacGillivray 1994; Iovino 2002), the Digitized Palomar Observatory Sky Survey (DPOSS) catalogue (Iovino et al. 2003; de Carvalho et al. 2005), and the Sloan Digital Sky Survey (SDSS) photometric catalogue DR1 (Lee et al. 2004) and DR6 (McConnachie et al. 2009). All of the above studies used only two-dimensional information of the galaxies (i.e. angular positions). Other CG catalogues were obtained by searches in redshift space: e.g. Barton et al. (1996) from the the CfA2 catalogue, Allam & Tucker (2000) from the Las Campanas Redshift Survey, Focardi & Kelm (2002) from the UZC Galaxy Catalogue, and Deng et al. (2008) from the SDSS-DR6 spectroscopic catalogue.

Since the nearly full spectroscopic followup by Hickson et al. (1992) of the original Hickson Compact Groups (HCGs; Hickson 1982), the velocity-filtered sample of 92 (69) HCGs with at least three (four) accordant-redshift members has been, by far, the most studied to date (e.g. Hickson, Kindl & Auman 1989 for optical photometry; Mendes de Oliveira & Hickson 1991 for galaxy morphologies; Moles et al. 1994; de la Rosa et al. 2007; Tzanavaris et al. 2010 for star formation rates; Coziol et al. 1998 for nuclear activity; de la Rosa, de Carvalho & Zepf 2001; Torres-Flores et al. 2010 for galaxy scaling relations; Verdes-Montenegro et al. 2001; Borthakur, Yun & Verdes-Montenegro 2010 for neutral gas content; Ponman et al. 1996 for hot gas content, etc.).

However, the visual inspection performed by Hickson (1982) led to a sample of CGs that is not reproducible, incomplete and not homogeneous (Hickson et al. 1989; Walke & Mamon 1989; Prandoni et al. 1994; Sulentic 1997; Díaz-Giménez & Mamon 2010). In particular, using the $z = 0$ outputs of semi-analytical models (SAM) of galaxy formation run on the Millennium cosmological dark matter simulation (Springel et al. 2005), Díaz-Giménez & Mamon (2010) have shown that the HCG sample is typically less than 10 per cent complete at the median distance of the sample.

The properties of CGs and their member galaxies must be studied using complete and well-defined observed samples. To achieve this goal, we present a new sample of automatically selected CGs extracted from the largest solid angle catalogue at present, the Two-Micron All-Sky Survey (2MASS). Using the 2MASS has two strong advantages: (1) it provides us with a full-sky survey and (2) the K-band photometry is only weakly sensitive to galactic extinction, internal extinction and recent star formation, and is thus a very good tracer of the stellar mass content of galaxies. For these reasons, it is ideal to build a CG sample from a wide K-band galaxy survey such as 2MASS (which has the additional benefit of being all-sky) with (nearly) full redshift information available from other sources (Mamon 1994).

The layout of this paper is as follows. In Section 2, we describe the parent catalogue. In Section 3, we present the CG catalogue. We perform a cross-identification between the 2MASS–CGs and other samples of groups in Section 4. In Section 5, we present a sample of CG after applying a velocity filtering, while we present some general properties of the samples in Section 6, and summarize and discuss our results in Section 7.

Throughout this paper we use a Hubble constant $H_0 = 100\,h\,\mathrm{km\,s^{-1}\,Mpc^{-1}}$, and for all cosmology-dependent calculations, we assume a flat cosmological model with a non-vanishing cosmological constant: $\Omega_\mathrm{m} = 0.25$ and $\Omega_\Lambda = 0.75$.

2 THE PARENT CATALOGUE: 2MASS XSC

The 2MASS survey (Skrutskie et al. 2006) has uniformly scanned the entire sky in three near-infrared bands to detect and characterize point sources brighter than about 1 mJy in each band, with signal-to-noise ratio (S/N) greater than 10. 2MASS used two highly automated 1.3-m telescopes, one at Mt. Hopkins, AZ, and one at Cerro Tololo InterAmerican Observatory, Chile. Each telescope was equipped with a three-channel camera, each channel consisting of a near infrared camera and multi object spectometer (NICMOS3) 256 × 256 HgCdTe array, capable of imaging a 8.5 × 8.5 arcmin^2 field at a pixel scale of 2 arcsec per pixel in the J (1.25 μm), H (1.65 μm) and K_s (2.17 μm) bands.

Our data set was selected from the publicly available, full-sky, extended source catalogue (XSC; Jarrett et al. 2000),[1] which contains over 1.6 million extended objects brighter than $K_s = 14.3$. We adopted the 'K20 isophotal fiducial elliptical aperture magnitudes' and selected galaxies that were neither flagged as artefacts (`cc_flg != 'a'`) nor close to large galaxies – thus avoiding spurious fragments in the envelopes of large galaxies (`cc_flg != 'z'`). There is a strong correlation between dust extinction and stellar density, which increases exponentially towards the Galactic Plane. Stellar density is a contaminant factor of the XSC since the reliability of separating stars from extended sources is very sensitive to this quantity (Jarrett et al. 2000). In order to avoid contamination from stars, we have constructed a mask for the 2MASS survey using the HEALPix (Górski et al. 2005) map with $N_\mathrm{side} = 256$ and excluding those pixels where the K_s-band extinction $A(K_s) = 0.367\,E(B - V) > 0.05$ and $|b| < 20$, which reduces galactic contaminant sources to 2 per cent (Maller et al. 2005). This filtering on galactic extinction reduced the solid angle from 27 334 deg^2 to 23 844 deg^2.

The raw magnitudes were corrected for galactic extinction using the reddening map of Schlegel, Finkbeiner & Davis (1998). We also followed Maller et al. and imposed a cut at $K_\mathrm{lim}^\mathrm{2MASS} = 13.57$ in the corrected magnitudes. The sky distribution of these galaxies is shown as the grey points in Fig. 1. These restrictions produced a sample of 408 618 extended sources which constitute our parent catalogue.

3 THE 2MASS CG CATALOGUE

We identify CGs in projection (*p2MCG*s) by using an automated searching algorithm very similar to that defined by Hickson (1982)

[1] http://irsa.ipac.caltech.edu/cgi-bin/Gator/nph-dd?catalog=fp_xsc

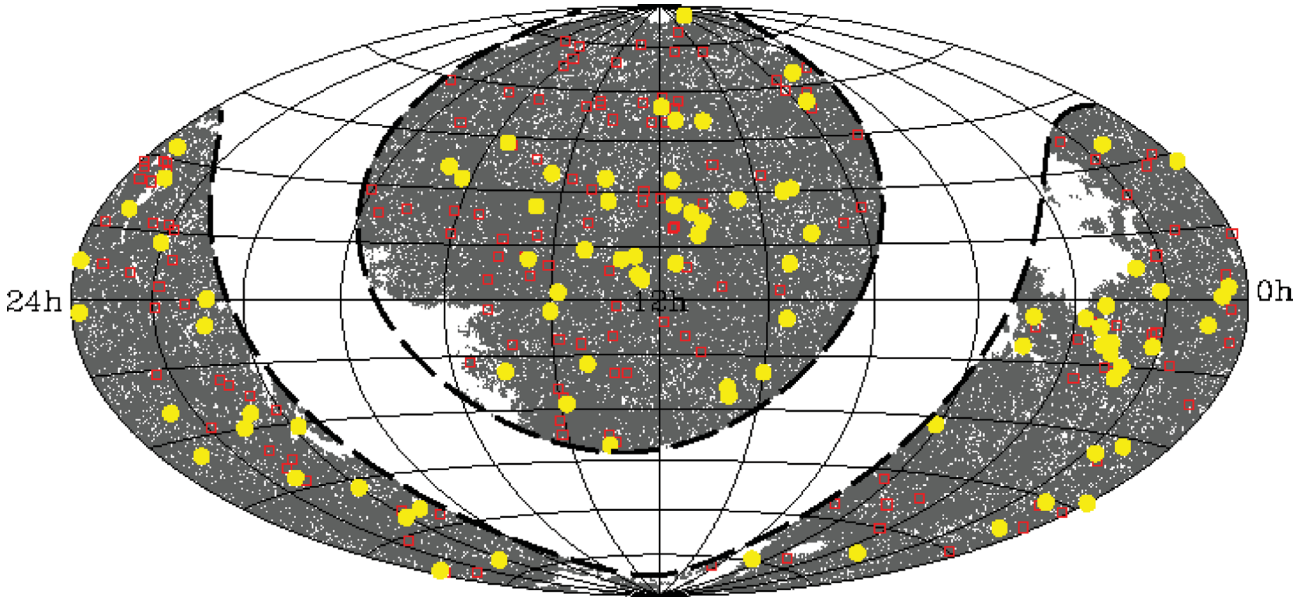

Figure 1. Aitoff projection of galaxies in the 2MASS XSC excluding the region $\pm 20^\circ$ around the Galactic Plane (*dashed lines*) and regions with high galactic extinction (*background points*). *Open squares* represent the 230 CGs identified in projection, while *filled circles* are the 85 CGs after the velocity filter.

which is fully described in Díaz-Giménez & Mamon (2010). Briefly, this algorithm identifies as *p2MCG*s those systems that satisfy the following criteria:

(i) $4 \leq N \leq 10$ (population)
(ii) $\mu_K \leq 23.6$ mag arcsec^{-2} (compactness)
(iii) $\theta_{\mathcal{N}} > 3\theta_{\rm G}$ (isolation)
(iv) $K_{\rm brightest} \leq K_{\rm lim}^{\rm 2MASS} - 3 = 10.57$ (flux limit)

where N is the total number of galaxies whose K-band magnitude satisfies $K < K_{\rm brightest} + 3$, and $K_{\rm brightest}$ is the apparent magnitude of the brightest galaxy of the group; μ_K is the mean K-band surface brightness, averaged over the smallest circle circumscribing the galaxy centres; $\theta_{\rm G}$ is the angular diameter of the smallest circumscribed circle, and $\theta_{\mathcal{N}}$ is the angular diameter of the largest concentric circle that contains no other galaxies within the considered magnitude range or brighter. Our compactness criterion is set to match that of the HCG, using a mean colour transformation of $K = R - 2.4$ (see Appendix A).

In order to speed up this computationally extensive algorithm, we used the subroutines of the HEALPix[2] package to find neighbours within 5° around each galaxy, and the STRIPACK[3] subroutines to compute the centres and radii of the minimum enclosing circles (hereafter CG centres and CG radii, respectively).

Using this algorithm, we found 262 *p2MCG*s in the 2MASS XSC, containing 1158 galaxies. We note, as a curiosity, that 3 ± 0.5 per cent (binomial errors) of our CGs with $N > 4$ contain a compact quartet core that also meets all the CG criteria. These are, in fact, CGs within CGs. Note that this percentage is significantly lower than the (6–13) per cent predicted by Díaz-Giménez & Mamon (2010) from the SAMs (with binomial uncertainty less than 0.5 per cent). Following Díaz-Giménez & Mamon, we always choose the larger CG.

Using the Aladin interactive sky atlas[4] (Bonnarel et al. 2000) and the Interactive 2MASS image server,[5] we performed a visual inspection of all of these *p2MCG*s. We found that there were 26 galaxy misidentifications in the 2MASS XSC: fragments of larger galaxies (often H II regions) or blends of two galaxies. In other words, since 26 galaxies are misidentifications over a total of 1158, then, for our purposes, the 2MASS XSC turned out to be 97.8 ± 0.4 per cent reliable. Fig. 2 shows a few examples of these misidentifications. In Table 1, we list the 26 objects that belonging to CGs were incorrectly classified as galaxies by 2MASS, and also are quoted the names of their host galaxies. We discarded those CGs of four members that hosted one of these galaxies. If a misidentified galaxy belonged to a CG with more than four members, then only this galaxy is discarded, and all properties of the CG are recomputed and all the criteria are checked again. In total, 20 groups were discarded because of incorrect 2MASS galaxy identifications.

Moreover, 2MASS fails to identify some large galaxies that are close to another large galaxy belonging to a CG. For instance, galaxy NGC 7578A does not appear in the 2MASS XSC, while its pair-neighbour, NGC 7578B, does. The same happened with the following 12 galaxies: NGC 0414-NED02, IC 0590-NED02, NGC 3750, NGC 4783, NGC 5354, NGC 4796, IC 1165 NED02, ESO 284-IG 041 NED02, ESO 596-49, LCRSB210329.4-450104, NGC 7318A and NGC 7318B. These 13 missing galaxies among 1158 detected ones make the 2MASS XSC 99 per cent complete for our purposes. Given the lack of K-band magnitudes for these galaxies, we omitted from our sample the 12 CGs containing these 13 galaxies.

As a result, we identify 230 *p2MCG*s in the 2MASS catalogue. In Fig. 1 we show the sky coverage of these groups (empty squares). Fig. 3 shows images of a few examples of *p2MCG*s that lie in the SDSS area. Some of the observable properties of the *p2MCG*s are shown in Fig. 4 and their median values are shown in the second column of Table 4.

[2] http://healpix.jpl.nasa.gov
[3] http://people.sc.fsu.edu/burkardt/f_src/stripack/stripack.html
[4] http://aladin.u-strasbg.fr/java/nph-aladin.pl
[5] http://irsa.ipac.caltech.edu/applications/2MASS/IM/interactive.html

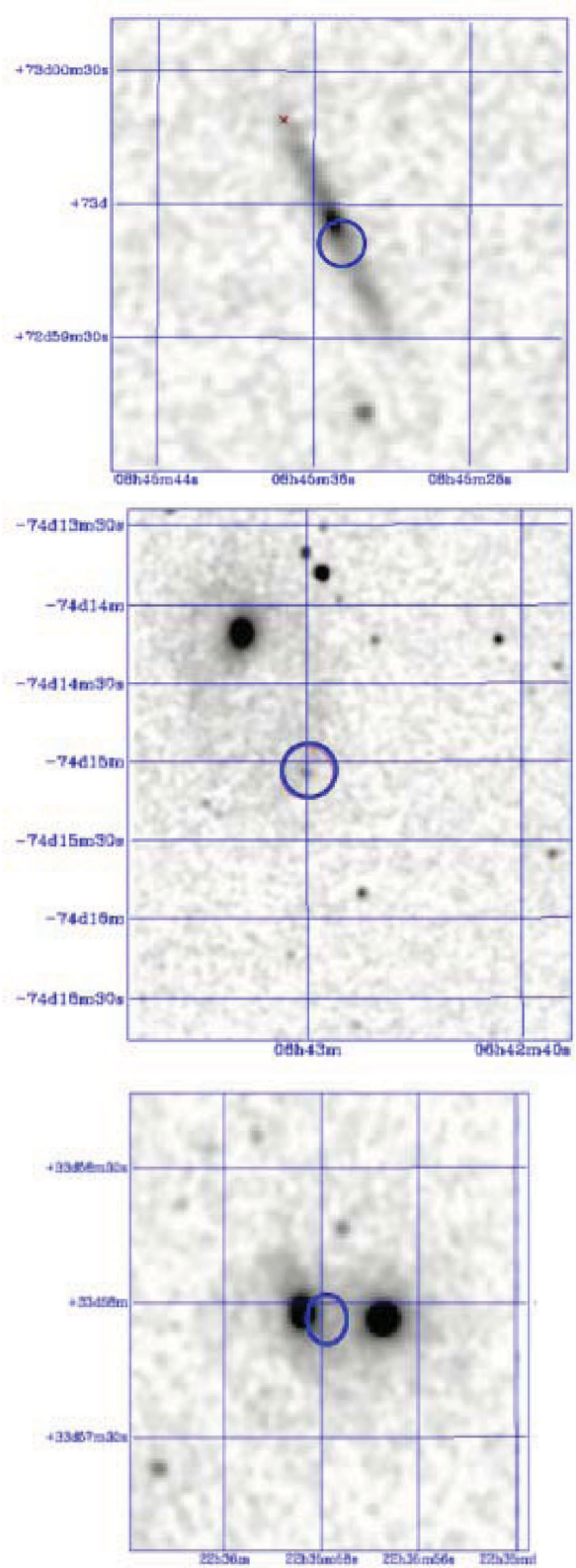

Figure 2. Images in the K_s band taken from the Interactive 2MASS Image Service showing 2MASS misidentification examples (see Table 1). Circles show the position of these objects in the 2MASS XSC. From top to bottom: 2MASXJ08453453+7259512, 2MASXJ06430003−7415042, 2MASXJ22355791+3357562. In all but the last image, the large galaxy close to the circles also belongs to 2MASS XSC.

Table 1. Objects in the 2MASS XSC that are actually part of larger galaxies.

No.	Galaxy name in 2MASS	Main galaxy
1	2MASXJ18533628−5643133	2MASXJ18533694−5643078
2	2MASXJ14080439−3318147	2MASXJ14080314−3318542
3	2MASXJ22355791+3357562	Galaxy pair
4	2MASXJ03554380−4222233	2MASXJ03554474−4222024
5	2MASXJ07271181+8544540	2MASXJ07271448+8545162
6	2MASXJ08453453+7259512	2MASXJ08453501+7259560
7	2MASXJ03582336−4428024	2MASXJ03582180−4427585
8	2MASXJ10421741−0022318	2MASXJ10421797−0022365
9	2MASXJ12422507−0702456	2MASXJ12422554−0702364
10	2MASXJ16013973+2121296	2MASXJ16014023+2121106
11	2MASXJ12040147+2013489	2MASXJ12040140+2013559
12	2MASXJ07222530+4916277	2MASXJ07222519+4916427
13	2MASXJ06430003−7415042	2MASXJ06430596−7414103
14	2MASXJ00364578+2134078	2MASXJ00364500+2133594
15	2MASXJ17465074+2045440	2MASXJ17465132+2045400
16	2MASXJ09054355+1820276	2MASXJ09054305+1820226
17	2MASXJ11282505+0924272	2MASXJ11282405+0924279
18	2MASXJ23223215+1153235	2MASXJ23223093+1153332
19	2MASXJ02142411−0722178	2MASXJ02142586−0722064
20	2MASXJ12214093+1129448	2MASXJ12214230+1130118
21	2MASXJ13193834−1242052	2MASXJ13193805−1241562
22	2MASXJ12494210+2653266	2MASXJ12494226+2653312
23	2MASXJ13561035+0514388	2MASXJ13560724+0515169
24	2MASXJ23535429+0757368	2MASXJ23535389+0758138
25	2MASXJ11561045+6031300	2MASXJ11561032+6031211
26	2MASXJ15375266+5923382	2MASXJ15375345+5923304

A list of acronyms used to refer different samples to be defined throughout this work is provided in Table 2.

4 CROSS-IDENTIFICATION

We compared our sample of CGs to the original HCG sample. We looked for the *K*-band magnitudes of all the original members of the HCG sample in the 2MASS catalogue. There are 42 HCGs that lie within the studied area (HCG 33 and 34 lie within 20° of the Galactic Plane) and whose brightest galaxy *K*-band magnitude is brighter than 10.57 (fourth criterion). However, only 20 HCGs have been identified with the *p2MCG*s in the 2MASS sample, and they are: HCG 4, 7, 10, 15, 16, 21, 22, 23, 25, 40, 42, 51, 58, 86, 87, 88, 93, 97, 99, 100. While 10 of these 20 CGs have the exact same member galaxies, the remaining 10 have galaxies in common but are not exactly the same: some groups have more galaxies unidentified by Hickson while others have fewer.

We therefore analysed the reasons why we failed to identify the 22 remaining HCGs among the 42. First, in HCG 68, HCG 92 (Stephan's quintet) and HCG 94, the 2MASS XSC photometric pipeline blends a pair of galaxies into a single galaxy or only identifies one galaxy of a pair. This then falls into the category of groups discarded due to problematic galaxy identification described in the previous section (in this case, galaxy NGC 5354 for HCG 68, galaxies NGC 7318A and NGC 7318B for Stephan's quintet, and NGC 7578A for HCG 94). Secondly, among the 19 remaining unidentified HCGs in our sample, 10 (HCG 5, 56, 57, 61, 65, 74, 90, 91, 96, 98) have less than four members within our adopted 2MASS limit of $K = 13.57$, i.e. some of their members do not belong to our parent sample. Moreover, HCG 57 also fails the HCG isolation criterion in the *R* band (Sulentic 1997), while HCG 74 and 96 fail the membership criterion in the *R* band. Finally, nine of the HCGs (HCG 11, 19, 30, 41, 44, 48, 53, 62, 67) fail to meet the *K*-band

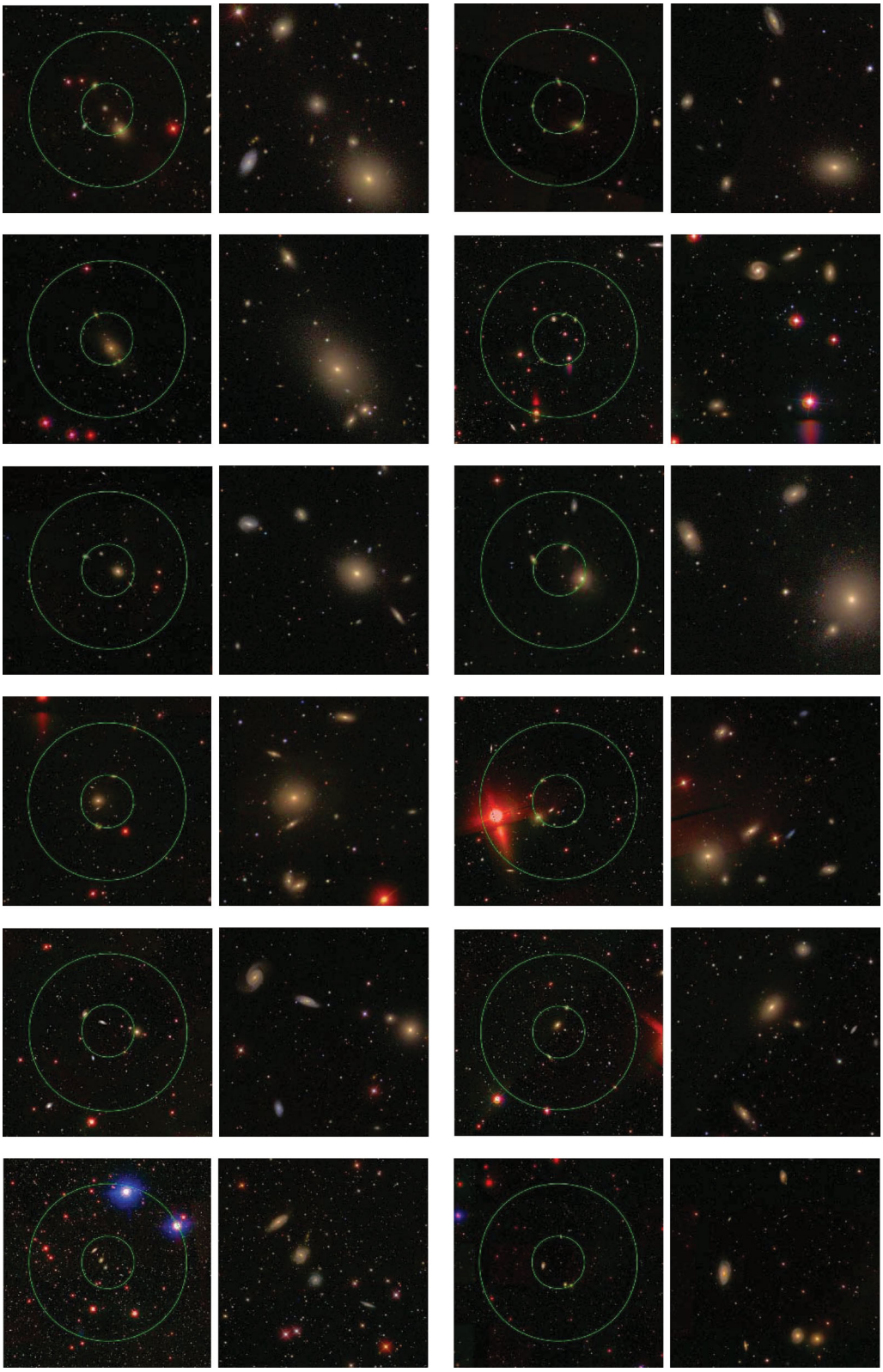

Figure 3. SDSS RGB images of A few examples of *p2MCG*s that lie within the SDSS area, none of them is an already known group. There are two frames per *p2MCG*: the *left frames* show concentric circles which correspond to 1 θ_G and 3 θ_G (see text). The *right frames* are zoomed images which show the regions within θ_G, for each group. According to the notation in Table C1 they are (from left to right and top to bottom): 32, 36, 40, 50, 52, 57, 59, 62, 64, 66, 74 and 85.

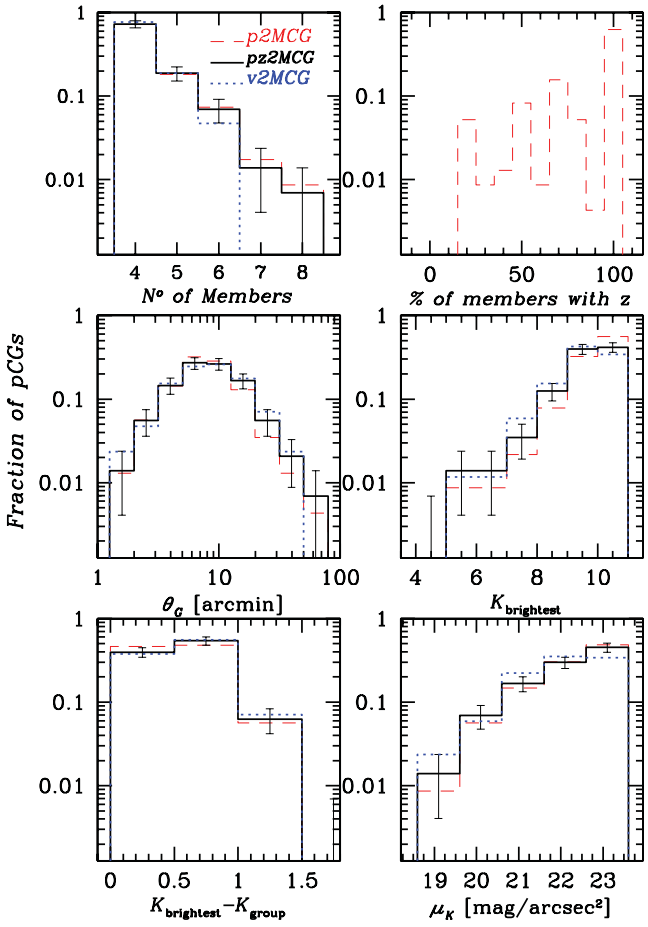

Figure 4. Distributions of observable properties for the CGs identified in projection in the 2MASS XSC: number of members in the CG (*top-left panel*), percentage of members with redshifts available (top-right panel), group angular diameter (*middle-left panel*), K-band apparent magnitude of the brightest galaxy member (*middle-right panel*), difference between the brightest galaxy and the total group magnitudes (*bottom-left panel*) and mean group surface brightness (*bottom-right panel*). Dashed histograms correspond to the sample of 230 *p2MCG*s, *solid histograms* correspond to the sample of 144 *p2MCG*s that have all the redshifts of their galaxies known (*pz2MCG*s), and will be filtered in Section 5, while *dotted histograms* correspond to the sample of 85 *v2MCG*s. Error bars correspond to Poisson errors.

Table 2. List of acronyms used throughout this work.

CG	General compact groups
p2MCG	CGs identified in projection from the 2MASS catalogue
pz2MCG	*p2MCG*s whose galaxies have their radial velocities known
v2MCG	CGs with four or more accordant galaxies (velocity filtered)
mvCG	Mock velocity-filtered CGs
HCG	Hickson Compact Groups

membership criterion, i.e. have fewer than four galaxies with $K - K_{\rm brightest} < 3$, one of which (HCG 30) also fails to meet this criterion in the R band.

The visual inspection performed using Aladin images has also provided information about other cross-identifications. Only 25 per cent of our *p2MCG*s have already been completely or partially identified by other authors.

5 VELOCITY-FILTERED COMPACT GROUPS

5.1 Velocity filtering

We searched in the literature for available redshifts for all galaxies in the *p2MCG* sample in order to have a sample of concordant groups. First, we correlated the galaxies in the 2MASS extended source catalogue with galaxies in the 2MASS Redshift catalogue (2MRS; Huchra et al. 2012). We have found 561 of our galaxies in *p2MCG*s in the main catalogue of those authors. Also, another 280 were present in the 'extra' catalogue presented by the authors. Then, we looked for the remaining galaxies in the 2M++ redshift compilation (Lavaux & Hudson 2011). We found nine of the remaining *p2MCG* galaxies in this catalogue. We also looked for available redshifts in the NASA/IPAC Extragalactic Database (NED) for those galaxies in the *p2MCG*s that do not belong to the 2MRS or to 2M++. We have found another 19 redshifts of galaxies in *p2MCG*s. All in all, we find that 869 out of 1020 galaxies (85 per cent) already have measurements of their redshifts available.

A total of 144 (62 per cent) of the *p2MCG*s have *all* their members with available redshifts, and we hereafter refer to these as *pz2MCG*s. In 20 per cent of the *p2MCG*s there is one galaxy without available redshift, while in 10 per cent (8 per cent) of the *p2MCG*s there are two (three or more) galaxies without redshifts.

Fig. 4 shows that the distributions of observable properties of the 144 *pz2MCG*s are very similar to those for the full sample of *p2MCG*s. Therefore, our subsample of *pz2MCG*s does not appear biased relative to the full sample of *p2MCG*s.

Using these 144 *pz2MCG*s, we built a sample of velocity-filtered CGs (*v2MCG*s) by following an iterative procedure (see Hickson et al. 1992; Díaz-Giménez & Mamon 2010). Briefly, after computing the median velocity of the group, we discard the galaxy whose velocity is furthest and at least $\Delta v = 1000\,{\rm km\,s^{-1}}$ from the median. We recompute the velocity median of the remaining galaxies and iterate until all, and at least four, galaxies lie within Δv from the new median. We then check that the brightest remaining galaxy is brighter than 10.57, and that $\mu_K \leq 23.6\,{\rm mag\,arcsec^{-2}}$. If not, we discard the group.

Our procedure led us to 85 *v2MCG*s that survive the velocity filtering, and are thus less likely to be contaminated by galaxies in chance projections. The angular distribution of these groups is shown in Fig. 1 (filled circles).

Fig. 5 shows the properties (see Section 5.3) of the *v2MCG*s (solid black histograms). One sees that the samples of *v2MCG*s appears to be complete up to $K_{\rm group} \simeq 9$, close to the theoretical limits for quartets ($10.57 - 2.5\log 4 = 9.06$) and the rarer quintets ($10.57 - 2.5\log 5 = 8.82$). The *v2MCG* sample also appears to be fairly complete[6] to radial velocity of $\sim$6000 km s^{-1}.

Fig. 4 displays a comparison between the sample of projected and filtered CGs. One sees that groups with higher multiplicity, or very large angular size, are more prone to be chance alignments along the line of sight.

5.2 Cross-identification

We found that 46 per cent of the *v2MCG*s were previously (completely or partially) identified by other authors (see the last column of Table C1). In particular, the *v2MCG*s include 16 HCGs: HCG 7,

[6] Of course, a flux-limited catalogue is never complete in terms of volume, since galaxies are sampled with increasing minimum luminosity as one goes out to increasing distances, hence the space density of galaxies always decreases (if it were not for fluctuations from the large-scale structure).

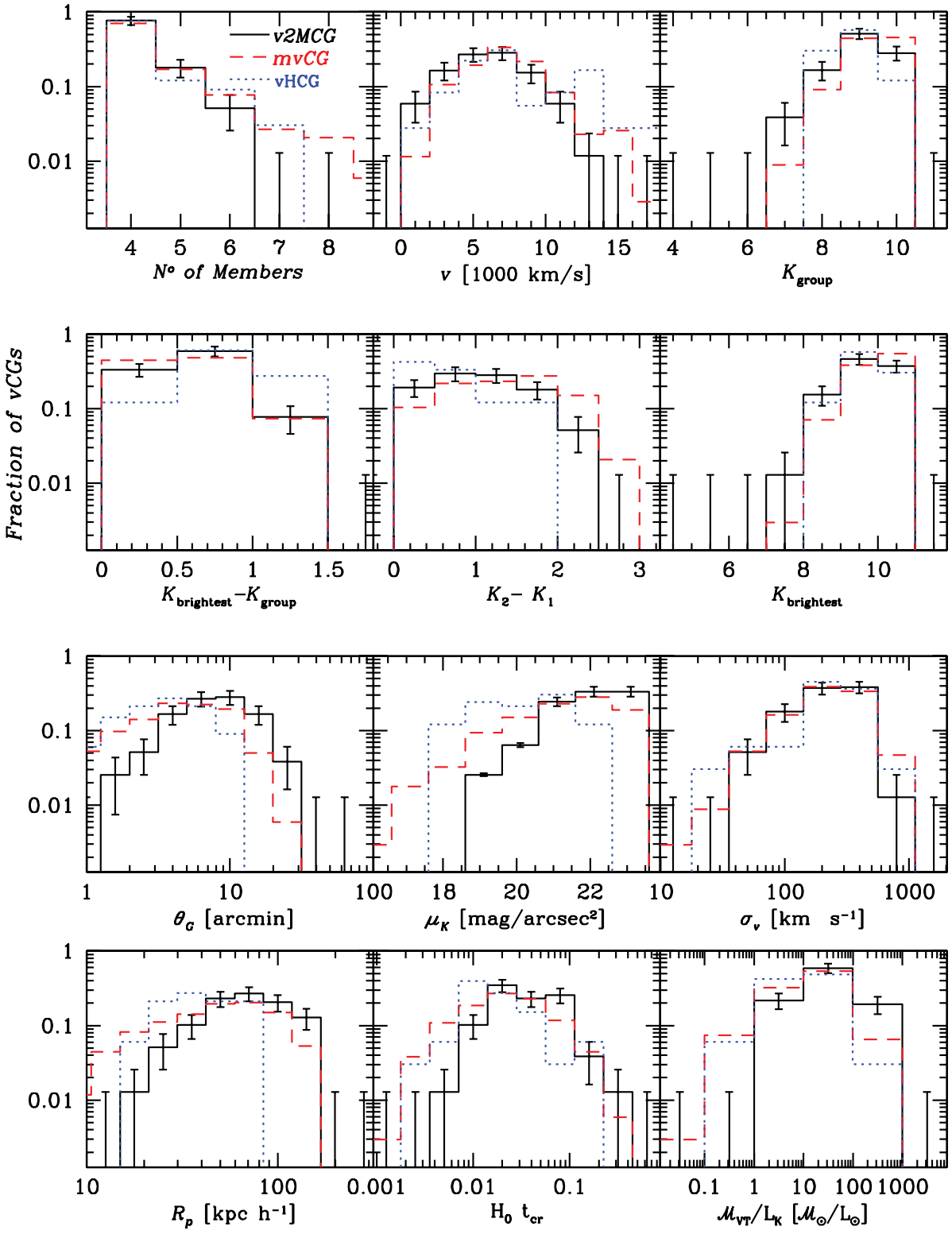

Figure 5. Distributions of properties of the CGs after the velocity filtering. All panels are restricted to groups with $\langle v \rangle > 3000\,\mathrm{km\,s^{-1}}$ except for the median group velocities. *Thick black solid histograms*: *v2MCGs*; *thin red dashed histograms*: velocity-filtered mock Compact Groups (*mvCGs*) identified in the *r* band from the SAM of Guo et al. (2011) run on the haloes of the MS-II dark matter simulation, and converted to the *K* band using $K = R - 2.4 = r - 2.73$ (Table 5); *thin blue dotted histograms*: vHCG are the velocity-filtered HCGs restricted to the limits used in this work and converted to the *K* band (sample Hick92/2, Table 5). Error bars correspond to Poisson errors.

10, 15, 16, 21, 23, 25, 40, 42, 51, 58, 86, 88, 93, 97 and 99. Moreover, 52 per cent of the *v2MCG*s lie in the SDSS area. The median of the properties are quoted in the second column of Table 5.

5.3 Measurement of group properties

The main properties of the *v2MCG*s are quoted in Table C1. They are:
Column 1: Group ID
Column 2: Right Ascension of the CG centre
Column 3: Declination of the CG centre
Column 4: Median radial velocity
Column 5: Number of galaxy members in the CG in the range of 3 mag from the brightest member
Column 6: Extinction-corrected K-band apparent magnitude of the brightest galaxy
Column 7: Extinction-corrected K-band group surface brightness
Column 8: Angular diameter of the smallest circumscribed circle
Column 9: Median projected separation among galaxies
Column 10: Apparent group elongation
Column 11: Radial velocity dispersion of the galaxies in the CG
Column 12: Dimensionless crossing time
Column 13: Mass-to-light ratio in the K band
Column 14: Cross-identification with other group catalogues.

The group velocity dispersions, $\sigma_{\rm v}$, are computed using the gapper algorithm following Beers, Flynn & Gebhardt (1990), who found it to be more efficient than standard estimators of dispersion for small samples.[7] Our values of $\sigma_{\rm v}$ are corrected (in quadrature) for the velocity errors.

The extinction corrections in Table C1 refer to the Galactic extinction, deduced from Schlegel et al. (1998). We did not correct for internal extinction, because the corrections are usually negligible, except for edge-on spirals where they are probably of the order of 0.2 mag. Moreover, we expect that internal extinction increases not only with the inclination of the disc, but also with disc luminosity (with increasing column density of dust at increasing luminosity for given dust/stars ratio) and metallicity (which controls the dust/stars ratio), as well as on the bulge/disc ratio. Since we lack bulge/disc decomposition for our galaxies, we could have used the internal extinction formulae for 2MASS wavebands of Masters, Giovanelli & Haynes (2003), given as a function of inclination and luminosity. However, their modulation of internal extinction by the luminosity saturates at luminosities of about $0.2\,L*$, whereas it should keep rising because, at increasing luminosity, the column density should increase and the metallicity, hence dust/stars ratio, should also increase. We thus prefer to leave the internal extinction to further analysis.

The physical radii and luminosities assume distances obtained from the redshifts, i.e. we neglect the peculiar velocities of the galaxies relative to the Sun. We could have included a Virgocentric infall model to correct for the peculiar velocity of the Local Group (as given in HyperLEDA;[8] see Terry, Paturel & Ekholm 2002), but this would not have included the peculiar motions of *v2MCG* galaxies. The attractor model of Mould et al. (2000) does include the peculiar motions of both the Local Group and the other galaxies, but it misses all the repelling voids. The peculiar velocity flow model of Lavaux et al. (2010) does include the full matter distribution and not just the attractors. But it was built from redshift data and lacks accuracy at distances less than $30\,h^{-1}$ Mpc because it is not calibrated with available quality distance estimators (Cepheids or surface brightness fluctuations). Since none of the models available satisfied our expectations taking into account all the main velocity components, we decided not to correct for peculiar motions, and we leave this open to further analysis. For peculiar velocities of $300\,{\rm km\,s^{-1}}$, the effects of peculiar motions on distances are less than 10 per cent for galaxies with $c\,z > 3000\,{\rm km\,s^{-1}}$ (leading to physical size and luminosity errors less than 10 per cent and 20 per cent, respectively). For the presentation and analysis of statistical *v2MCG* properties, we thus restrict our sample to the 78 *v2MCG*s for which the median group velocity is greater than $3000\,{\rm km\,s^{-1}}$.

We compute the absolute magnitudes of the individual galaxies, assuming that their luminosity distances are all based upon the median group redshift. The cosmology adopted for computing the luminosity distances is the standard cosmology also used in the MS ($\Omega_{\rm m} = 0.25$, $\Omega_\Lambda = 0.75$). Note that the luminosities are not only corrected for galactic extinction, but are also k-corrected. For computing the k-corrections, we have used the polynomial expressions in terms of redshift and colour $H - K$ given by Chilingarian, Melchior & Zolotukhin (2010). The results of the present work depend very little on the details of the k-corrections, since the galaxy samples studied here are from shallow flux-limited surveys, hence limited to low redshifts.

Our dimensionless crossing times are obtained with

$$H_0\,t_{\rm cr} = H_0\,\frac{\left\langle d_{ij}^{3D}\right\rangle}{\sigma_{\rm 3D}} = \frac{100\,\pi}{2\sqrt{3}}\,h\,\frac{\langle d_{ij}\rangle}{\sigma_{\rm v}}, \qquad (1)$$

where $\langle d_{ij}\rangle$ is the median of the inter-galaxy projected separations in h^{-1} Mpc. Our mass-to-light ratios are obtained from an application of the virial theorem:

$$\frac{\mathcal{M}_{\rm VT}}{L} = \frac{3\pi}{2}\,\frac{(2\,R_{\rm h})\,\sigma_{\rm v}^2}{G\,L}, \qquad (2)$$

where $R_{\rm h} = \langle 1/d_{ij}\rangle^{-1}$ is the harmonic mean projected separation, given the projected separations d_{ij} (see equations 10– 23 of Binney & Tremaine 1987).

The distributions of the main properties of the *v2MCG*s are shown as solid black histograms in Fig. 5.

5.4 Mock velocity-filtered compact groups

It is instructive to compare the distribution of the properties of *v2MCG*s with the mock, velocity-filtered compact groups (*mvCG*s) selected on mock galaxy catalogues with the exact same criteria as those described at the top of Section 3. We have done this following the prescriptions of Díaz-Giménez & Mamon (2010), who had analysed the $z = 0$ outputs of three different SAMs of galaxy formation (Bower et al. 2006, hereafter B06; Croton et al. 2006, hereafter C06; De Lucia & Blaizot 2007, hereafter DLB07).

However, since this work, a new SAM has been developed by Guo et al. (2011) (hereafter G11) that reproduces much better, among other things, the $z = 0$ stellar mass function of galaxies. Moreover, G11 have run their SAM not only on the Millennium dark matter simulation, but also on the Millennium-II simulation (MS-II; see Boylan-Kolchin et al. 2009), which has five times better space resolution and 125 times better mass resolution. Since CGs are small, space and mass resolution are crucial in producing realistic mock CG catalogues. We have therefore primarily used the outputs of the G11 SAM run on top of the MS-II to build realistic mock light cones to a magnitude limit of $r = 16.3$ (the limit of the 2MASS

[7] One of us (GAM, unpublished) also found the gapper estimate of dispersion to be much less biased for small samples than are other measures.
[8] http://leda.univ-lyon1.fr/

Table 3. Mock velocity-filtered CGs.

Parent ΛCDM simulation	MS	MS	MS	MS	MS-II
SAM	B06	C06	DLB07	C06K	G11
Selection band	*R*	*R*	*R*	*K*	*r*
$R_{\rm brightest} \leq 14.44$ & $\mu_R \leq 26$					
Number of *mvCG*s	1952	2011	1251	–	1782
Fraction of physically dense	0.77	0.73	0.58	–	0.69
$K_{\rm brightest} \leq 10.57$ & $\mu_K \leq 23.6$					
Number of *mvCG*s	379	360	288	486	340
Fraction of physically dense	0.73	0.65	0.53	0.66	0.66

Note. MS, Millennium Simulation (Springel et al. 2005); MS-II, Millennium-II Simulation (Boylan-Kolchin et al. 2009); B06, Bower et al. (2006); C06, Croton et al. (2006); DLB07, De Lucia & Blaizot (2007); G11, Guo et al. (2011).

converted to the SDSS *r* band) and identify CGs. We have also reanalysed the $z = 0$ output of the SAM by C06, this time using their *K*-band magnitudes instead of the *R*-band ones to a magnitude limit of $K = 13.57$ (the 2MASS completeness limit used throughout this work). We refer to these *mvCG*s as C06K. Note that, as in Díaz-Giménez & Mamon (2010), we assumed for all SAMs that mock galaxies that are close in projection on the plane of the mock sky would be blended by observers if their angular separation is less than the sum of their angular half-light radii.

Table 3 shows the fraction of *mvCG*s, selected in redshift space as the observed catalogues, that are physically dense in real space with the criteria adopted by Díaz-Giménez & Mamon (2010). Here, *s* the maximum pair separation in real space among the closest subsample of four galaxies of the CG or the CG itself for quartets, while $S_\perp$ and $S_\parallel$ denote the maximum line of sight and projected separations of the subsample, respectively. With these notations, the criterion for physically dense groups is that they be physically very small or that they be physically small and not elongated along the line of sight: ($s < 100\,h^{-1}$ kpc) *OR* ($s < 200\,h^{-1}$ kpc *AND* $S_\parallel/S_\perp < 2$). Assuming that the predictions from the SAM can be directly applied to the *v2MCG*s, we predict that between ∼53 and ∼73 per cent of the sample can be considered as physically dense systems, which means that between ∼45 and ∼62 *v2MCG*s may be truly dense systems. The remaining 37 ± 10 per cent of the *mvCG*s are caused by chance alignments of galaxies along the line of sight, usually originating from larger virialized groups (see also Díaz-Giménez & Mamon 2010).

In particular, for the more realistic G11 SAM run on the much better resolved MS-II cosmological dark matter simulation, *two-thirds of the mock velocity-filtered CGs are physically dense*, while one-third is caused by chance alignments of galaxies along the line of sight, mostly within larger virialized groups. So, this better SAM produces a fraction of mock velocity-filtered CGs that are physically dense that is similar to what Díaz-Giménez & Mamon (2010) had found for the three other SAMs. Comparing the upper and lower rows of Table 3, it is encouraging that the fraction of physically dense *mvCG*s depends little on the waveband (red or *K*) used.

6 GENERAL PROPERTIES

It is interesting to compare the properties of the CGs presented in this work to those found in the literature for other CG samples. We downloaded several CG catalogues available at the VizieR service[9] of the Centre de Données astronomiques of Strasbourg (CDS), and computed the properties of these groups in the same way we did for our sample of CGs.

6.1 Comparison with photometric catalogues

We retrieved data from VizieR for the following six catalogues: HCG (Hickson 1982), DPOSSCG/03 (Iovino et al. 2003), DPOSSCG/05 (de Carvalho et al. 2005), SDSSCG/04 (Lee et al. 2004), SDSSCG-A/09 (McConnachie et al. 2009) and SDSSCG-B/09 (McConnachie et al. 2009). It is important to note that, although we used the membership information from the authors (angular positions and magnitudes), we recomputed all the properties using our own algorithms, to ensure that they were all estimated in the same manner. In this way, we can compare our projected *p2MCG* catalogue with others in the literature to highlight differences in the searching algorithms and selection criteria.

Table 4 shows the median observable properties and their interquartile ranges for the photometric samples of CGs. For a fair comparison among these samples, it is necessary to take into account the different bands in which CGs have been identified in each different catalogue. While our *p2MCG*s are based upon *K*-band magnitudes, HCGs have been first identified on POSS-I *E* plates, whose spectral response is close to the *R* band, for which the galaxy magnitudes are available. DPOSSCG/03 have SDSS-*r* band magnitudes, DPOSSCG/05 have *R*-Gunn magnitudes, and SDSSCG/04/09 have SDSS-*r* band magnitudes. We assumed that $R = K + 2.4$ (appendix A) and $R = r - 0.33$ (Díaz-Giménez & Mamon 2010) to compare magnitudes in the *K* and *r* band to those in the *R* band. Therefore, in Table 4, all magnitudes are converted to the *R* band. Table 4 also includes a cleaner subsample of the HCG (Hick82/2) that meets equivalent criteria as that used in this work ($R_{\rm brightest} \leq 10.57 + 2.4 = 12.97$ and $R_{\rm faintest} - R_{\rm brightest} \leq 3$) and for which we omitted six HCGs that fail to meet the isolation criterion (Sulentic 1997) (see also thin dotted blue lines in Fig. 5).

Table 4 indicates that the *p2MCG*s have brighter group and first-ranked galaxy apparent magnitudes than those of the other photometric catalogues. This is a consequence of the shallower magnitude limit of the 2MRS spectroscopic survey used here. Restricting the HCG sample to the magnitude limits used here ('Hick82/2'), the median first-ranked galaxy magnitude is slightly brighter than that of the *p2MCG*s. The differences remaining between the *p2MCG* and Hick82/2 samples arise from the differences between automatic and visual identifications, since the latter by Hickson (1982) were biased (e.g., Díaz-Giménez & Mamon 2010) towards identifying groups with similar galaxies (lower values of $R_{\rm faintest} - R_{\rm brightest}$, and higher values of $R_{\rm brightest} - R_{\rm G}$), and missing groups close to the compactness limit (higher values of $\mu_{\rm G}$). On the other hand, the median angular diameter of the *p2MCG*s is larger than for the other samples, making the surface brightness of our sample the faintest. Moreover, not all the CG catalogues were constructed taking into account our fourth criterion that ensures that group members can be found in a 3 mag range from the first-ranked galaxy. In several of the catalogues, the magnitude limit of the sample is sometimes just 1 or 2 mag fainter than that of the first-ranked galaxy. It is clear that this leads to a bias towards identification of smaller differences between the first-ranked and faintest member of the group, as can be seen, e.g., in the average values of $R_{\rm faintest} - R_{\rm brightest}$ of 1.6 for the DPOSS/03/05 and SDSSCG-A/B catalogues.

It is interesting to compare the number of *p2MCG*s with $\delta > -33^\circ$ and $K_{\rm brightest} < 10.57$ with the number of HCGs in the same range of magnitudes. We find 193 *p2MCG*s versus 40 *pHCG*s that meet the

[9] http://vizier.u-strasbg.fr

Table 4. Median properties of CGs identified in projection. For a fair comparison, all photometric properties have been translated to the *R* band.

	p2MCG	HCG	DPOSSCG/03	DPOSSCG/05	SDSSCG/04	SDSSCG-A/09	SDSSCG-B/09	HCG
Ref.		Hick82	Iov03	deCarv05	Lee04	McCon09	McCon9	Hick82/2
Colour eq.	$K = R$–2.4	$E = R$	$r = R$+0.33	R	$r = R$+0.33	$r = R$+0.33	$r = R$+0.33	$E = R$
No.	230	100	84	459	177	2297	74791	40
θ_G (arcmin)	7.6 ± 2.8	3.1 ± 1.4	0.7 ± 0.1	0.7 ± 0.1	0.4 ± 0.1	1.5 ± 0.4	0.4 ± 0.1	4.4 ± 1.8
$R_{\rm brightest}$	12.5 ± 0.4	12.7 ± 0.6	16.2 ± 0.2	16.5 ± 0.3	16.8 ± 0.6	15.8 ± 0.5	18.4 ± 0.7	12.3 ± 0.6
R_G	11.9 ± 0.5	11.9 ± 0.6	15.3 ± 0.3	15.6 ± 0.3	16.2 ± 0.5	15.0 ± 0.4	17.6 ± 0.5	11.3 ± 0.6
μ_G (R mag arcsec^{-2})	25.0 ± 0.7	22.8 ± 0.7	23.1 ± 0.3	23.6 ± 0.3	23.2 ± 0.3	24.5 ± 0.6	24.5 ± 0.5	23.2 ± 0.8
$R_{\rm faintest}$–$R_{\rm brightest}$	2.7 ± 0.2	2.4 ± 0.5	1.6 ± 0.3	1.6 ± 0.3	2.7 ± 0.2	1.6 ± 0.5	1.9 ± 0.6	2.2 ± 0.4
$R_{\rm brightest}$–R_G	0.5 ± 0.2	0.9 ± 0.2	0.9 ± 0.2	0.9 ± 0.1	0.5 ± 0.2	0.9 ± 0.2	0.8 ± 0.2	0.9 ± 0.2

Note. θ_G, group angular diameter; $R_{\rm brightest}$, apparent magnitude of the brightest galaxy member in the *R* band; R_G, total apparent magnitude of the group (i.e. sum of all members); μ_G, group mean surface brightness; $R_{\rm faintest} - R_{\rm brightest}$, difference of apparent magnitudes between the faintest and the brightest galaxy members; $R_{\rm brightest} - R_G$, difference between the brightest galaxy and the total apparent magnitudes of the groups. Errors are the semi-interquartile ranges. References: Hick82: Hickson (1982); Iov03: Iovino et al. (2003); deCarv05: de Carvalho et al. (2005); Lee04: Lee et al. (2004); McCon09: McConnachie et al. (2009); Hick82/2: Hickson (1982), restricted to $R_{\rm brightest} \leq 10.57 + 2.4 = 12.97$ and $R_{\rm faintest} - R_{\rm brightest} \leq 3$ and with non-isolated groups (Sulentic 1997) removed.

criteria used in this work translated to the *R* band ($K_{\rm brightest} \leq 10.57$ and $K_i - K_{\rm brightest} \leq 3$), which means that the completeness of the visually identified HCGs is $\sim$21 $\pm$ 2 per cent (binomial errors). This result is higher than the 14 per cent predicted by Díaz-Giménez & Mamon (2010) from the semi-analytic models of galaxy formation. Moreover, in our analysis of the SAM of C06, identifying in the deeper *R*-band mock catalogue and then translating to the *K* band produce a sample of *mvCG*s that is only 74 per cent of the size of the *mvCG* sample directly selected in *K*. Thus, the incompleteness of the HCG catalogue relative to the 2MCG one is $0.21/0.74 = 0.28$, even higher than the prediction from the SAMs in the *R* band.

Given that the properties shown in Table 4 are dependent on the distances to the CGs, which are not included in the analysis above, it is also interesting to compare catalogues for which velocity information is available. This is done in the following subsection.

6.2 Comparison with observed and mock spectroscopic catalogues

We retrieved galaxy data from VizieR for the following CG catalogues with velocity information: HCG (Hickson et al. 1992), UZC-CG (Focardi & Kelm 2002) and Las Campanas Compact Groups (LCCG) (Allam & Tucker 2000). We also extracted the group information from the new DPOSSII-CG catalogue (Pompei & Iovino 2012). We then proceeded to compare those samples to our *v2MCG* sample, after transforming again all samples to the *R* band with colours $R - K = 2.4$ (Appendix A), $B = R + 1.7$ (Prandoni et al. 1994) and $r = R + 0.33$ (Díaz-Giménez & Mamon 2010). We have applied *k*-corrections to the different catalogues using the morphology-based corrections of Poggianti (1997) (UZC-CG and LCCG) or colour-based corrections of Chilingarian et al. (2010) (*v2MCG*, HCG).[10] We have included the cleaner Hick92/2 subsample (see Section 6.1) now velocity filtered, and also the sample of *mvCG*s that we extracted from G11's SAM. The median values of the properties of the velocity-filtered CGs are quoted in Table 5 as well as their semi-interquartile ranges.

6.2.1 *Space density*

We computed the space density within the median distance of the sample ($60\,h^{-1}$ Mpc) as $\eta_{60} = 3\,N(<60)/(60^3\Omega)$. For the *v2MCG*s the space density is $8.0 \times 10^{-5}\,h^3\,{\rm Mpc}^{-3}$. In comparison, the space density for the Hick92/2 sample is $1.86 \times 10^{-5}\,h^3\,{\rm Mpc}^{-3}$, i.e. that the space density of the *v2MCG*s is $\sim$4.3 times larger. From the G11 SAM, the space density of the *mvCG*s is $12.7 \times 10^{-5}\,h^3\,{\rm Mpc}^{-3}$, which means that it almost doubles ($\sim$1.6) that of the *v2MCG*s.

6.2.2 *Distribution of group properties*

In Fig. 5, we show the distribution of group properties for our *v2MCG*s (solid histograms), *vHCG*s (blue dotted histograms) and the *mvCG*s from G11 (thin dashed red histograms). The comparison with other SAMs can be found in Appendix B.[11] Table 5 shows that the nearest samples are the UZC-CG and *v2MCG* samples, although the HCG sample restricted to the criteria used in this work also includes only the nearest groups. The two nearby CG samples present the largest projected radii, median inter-particle distances, dimensionless crossing times and mass-to-light ratios. The five CG samples have similar median properties (to within the semi-interquartile ranges), except for T_1 and T_2 (see below). In particular, the median velocity dispersions for the different catalogues are fairly similar, ranging from 194 to 295 km s^{-1}.

Our sample has the highest median crossing time of all samples, while the HCG has the lowest crossing time. The latter result is probably caused by the lack of HCGs near the surface brightness limit (Walke & Mamon 1989; Prandoni et al. 1994; Díaz-Giménez & Mamon 2010).

There is a good general agreement between the predictions from the SAM and the observations from 2MASS. But some differences stand out (as checked with a Kolmogorov–Smirnov (KS) test on the full *N* distributions) in comparison with the *mvCG*s, the *v2MCG* sample lacks groups of high-multiplicity, very low velocity dispersion, small angular and physical sizes, high surface brightness, and low $\mathcal{M}_{\rm VT}/L_K$, but has too many groups that lie at low redshifts, or

[10] We did not apply *k*-corrections to DPOSSII-CG because of the lack of galaxy information, and we corrected their crossing time definition to ours ($\pi^2/9 \simeq 1.2$ times greater).

[11] Given that the numbers of *mvCG*s from the different SAMs are typically four times the number of *v2MCG*s, the relative uncertainties on their differential distribution is half of those of the *v2MCG*s, and are not shown in the figure for clarity.

Table 5. Median properties of CGs after velocity filtering, with radial velocity larger than 3000 km s^{-1}.

	v2MCG	HCG	UZC-CG	LCCG	DPOSSII-CG	HCG	*mvCG*
Ref.		Hick92	Foc02	Allam00	Pom12	Hick92/2	G11
Colour equation	$K = R$–2.4	$E = R$	$B = R$+1.7	R	$B = R$+1.7	$E = R$	$r = R + 0.33$
No.	78	67	49	17	33	33	326
θ_G (arcmin)	7.7 ± 3.1	2.5 ± 1.3	11.8 ± 4.2	1.0 ± 0.3	–	3.6 ± 1.5	4.8 ± 2.8
$R_{\rm brightest}$	12.2 ± 0.4	12.7 ± 0.6	12.6 ± 0.5	16.1 ± 0.4	–	12.2 ± 0.5	12.4 ± 0.4
R_G	11.5 ± 0.5	11.9 ± 0.7	11.3 ± 0.5	15.1 ± 0.3	–	11.3 ± 0.5	11.8 ± 0.4
μ_G (mag arcsec^{-2})	24.5 ± 0.7	22.7 ± 0.6	25.5 ± 0.6	23.9 ± 0.6	–	22.7 ± 0.9	23.9 ± 1.1
$R_{\rm faintest} - R_{\rm brightest}$	2.5 ± 0.3	2.1 ± 0.5	1.2 ± 0.4	1.2 ± 0.5	–	2.2 ± 0.4	2.7 ± 0.2
$R_{\rm brightest} - R_G$	0.6 ± 0.2	0.9 ± 0.2	1.2 ± 0.4	1.1 ± 0.2	–	0.8 ± 0.2	0.6 ± 0.2
$R_2 - R_1$	1.0 ± 0.4	0.6 ± 0.4	0.4 ± 0.4	0.5 ± 0.3	–	0.6 ± 0.4	1.3 ± 0.5
$L_R/10^{10}(h^{-2}\,L_\odot)$	6.7 ± 1.7	11.5 ± 5.1	7.1 ± 2.6	3.0 ± 0.7	4.2 ± 1.0	12.6 ± 5.1	6.7 ± 2.2
v (km s^{-1})	6361 ± 1680	9248 ± 2976	6287 ± 1380	23599 ± 3715	32321 ± 5522	7042 ± 3191	7023 ± 1471
σ_v (km s^{-1})	237 ± 105	262 ± 93	298 ± 99	243 ± 103	194 ± 55	271 ± 78	248 ± 115
$\langle d_{ij} \rangle$ (h^{-1} kpc)	86 ± 24	43 ± 15	132 ± 34	42 ± 5	31 ± 6	47 ± 15	59 ± 28
r_p (h^{-1} kpc)	65 ± 25	34 ± 12	108 ± 27	35 ± 6	–	36 ± 12	48 ± 23
b/a	0.43 ± 0.17	0.37 ± 0.17	0.47 ± 0.19	0.37 ± 0.16	–	0.37 ± 0.15	0.40 ± 0.18
$H_0\,t_{\rm cr}$	0.032 ± 0.024	0.013 ± 0.008	0.039 ± 0.024	0.014 ± 0.008	0.018 ± 0.005	0.016 ± 0.008	0.020 ± 0.017
$\mathcal{M}_{\rm VT}/L_R$ ($h\,\mathcal{M}_\odot/L_\odot$)	116 ± 42	42 ± 28	235 ± 193	117 ± 76	94 ± 34	39 ± 20	53^{+91}_{-32}
T_1	0.51 ± 0.06	1.27 ± 0.17	1.04 ± 0.15	1.10 ± 0.27	–	1.15 ± 0.22	0.46 ± 0.02
T_2	0.70 ± 0.06	1.01 ± 0.10	1.13 ± 0.11	1.10 ± 0.19	–	0.98 ± 0.13	0.59 ± 0.02
P_S	3×10^{-4}	0.19	0.53	0.86	–	0.31	0
P_{KS}^{1-2}	9×10^{-4}	(0.40)	0.09	(0.93)	–	(0.08)	5×10^{-10}
P_{KS}^{2-3}	(0.90)	(0.69)	(0.23)	(0.93)	–	0.25	(0.38)

*Note.*All the photometric properties have been translated to the R band to allow comparison among catalogues. No.: number of CGs with four of more concordant members; θ_G: group angular diameter; $R_{\rm brightest}$: apparent magnitude of the brightest galaxy member in the R band; R_G: total apparent magnitude; μ_G: group mean surface brightness; $R_{\rm faintest} - R_{\rm brightest}$: difference of apparent magnitudes between the faintest and the brightest galaxy members; $R_{\rm brightest} - R_G$: difference between the brightest galaxy and the total apparent magnitudes; $R_2 - R_1$: difference of absolute magnitudes between the brightest and the second brightest galaxy of the group (same statistics for difference in absolute R-band magnitudes, after including k-corrections from Chilingarian et al. 2010 and Poggianti 1997); L_G: total luminosity of the CG; v: group median radial velocity; σ_v: group gapper (Wainer & Thissen 1976) velocity dispersion, corrected for galaxy velocity errors (assumed to be 40 km s^{-1} when unavailable); $\langle d_{ij} \rangle$: median inter-galaxy separation; r_p: group radius (of smallest circumscribed circle); b/a: apparent elongation of the group (1 = round); $H_0\,t_{\rm cr}$: dimensionless crossing time (equation 1); $\mathcal{M}_{\rm VT}/L_R$: mass-to-R-light ratio from the virial theorem (equation 2); T_1 and T_2: Tremaine–Richstone statistics (Tremaine & Richstone 1977, equation 3); P_S: probability of greater anti-correlation of luminosity with position occurring by chance (Spearman rank correlation test); P_{KS}^{1-2}: probability of greater difference in distributions of positions between first and second ranked galaxies, occurring by chance (KS test); P_{KS}^{2-3}: same for difference in distribution of positions between second and third ranked galaxies. Numbers in parentheses for these three quantities indicate reverse luminosity segregation (brighter galaxies further out). Errors are the semi-interquartile ranges, except for T_1 and T_2, where they are standard deviations computed with 10 000 bootstraps. References: Hick92: Hickson et al. (1992); Foc02: Focardi & Kelm (2002); Allam00: Allam & Tucker (2000); Pom12: Pompei & Iovino (2012), restricted to isolated (classes A, CH and CP) with at least four accordant redshifts; Hick92/2: Hickson et al. (1992), restricted to isolated groups (following Sulentic 1997) and restricted to $R_{\rm brightest} \leq 10.57 + 2.4 = 12.97$ and $R_{\rm faintest} - R_{\rm brightest} \leq 3$; G11: mock CGs extracted (following the method of Díaz-Giménez & Mamon 2010) from the mock galaxy catalogue of G11 applied to the MS-II (Boylan-Kolchin et al. 2009) cosmological N-body simulation.

that are globally bright ($K_{\rm group}$) or with bright first-ranked galaxy ($K_{\rm brightest}$).

Our identification of more *v2MCG*s at low redshifts than predicted by the SAM might be a sign that our local neighbourhood ($c\,z < 2000$ km s^{-1}) is denser than on average, perhaps thanks to the presence of the Virgo and Fornax clusters, or conversely that the observer we placed in a random position in the cosmological box turned out to be in an underdense region (for small volumes one might expect that cosmic variance is then Poisson variance). This excess of nearby CGs would explain our excess of *v2MCG*s with large angular size and of low surface brightness. However, we also find an excess in physical radii, which suggests that we suffer more from galaxy blending than we accounted for in our *mvCG*s.

6.2.3 *Apparent group elongations*

Using projected Cartesian coordinates on the plane of the sky, we calculated the two-dimensional shape tensor, whose eigenvalues are related to the major (a) and minor (b) semi-axes. We measure the elongations of the groups in the plane of the sky as the ratio between the major and minor semi-axes (b/a). Lower values of b/a imply more elongated systems on the plane of the sky. Table 5 indicates that the apparent group elongations are similar between all catalogues.

Using a different technique to measure group apparent elongations, Tovmassian, Martinez & Tiersch (1999) found that group velocity dispersions were significantly smaller (by 28 per cent, with large uncertainty) in chain-like groups than in rounder ones, which we hereafter denote as the Tovmassian effect. Now, geometrical considerations imply that the distribution of group shapes depends on the number of its members (e.g. Hickson et al. 1984), with low multiplicity groups being on average more elongated. Since velocity dispersion scales as mass, which scales as number, one would then expect from the geometrical considerations that high-velocity dispersion groups will be rounder, as found by Tovmassian et al. However, these authors also noticed trends for triplets, quartets and quintets separately, and while none was statistically significant, they

Table 6. Group (quartets) velocity dispersion versus apparent elongation.

Catalogue	r	P_S	$\langle\sigma_v^{chain}\rangle$ (km s^{-1})	$\langle\sigma_v^{round}\rangle$ (km s^{-1})	P_{KS}
v2MCG	0.01	0.95	204	188	0.50
HCG (Hick92/2)	0.20	0.33	149	284	0.19
mvCG-G11	0.11	0.11	208	272	0.09
mvCG-C06	0.01	0.85	240	209	0.94
mvCG-B06	0.04	0.54	227	240	0.75
mvCG-DLB07	0.02	0.81	290	274	0.99
mvCG-C06K	0.10	0.10	240	280	0.10

Note. The samples are those listed in Table 5, hence limited to $v > 3000$ km s^{-1}, but also restricted to quartets ($N = 4$). The columns are r: Spearman rank correlation coefficient; P_S: probability of stronger correlation than r occurring by chance; $\langle\sigma_v^{chain}\rangle$ and $\langle\sigma_v^{round}\rangle$: median group velocity dispersions for chain-like ($b/a < 0.3$) and round ($b/a > 0.5$) groups, respectively; P_{KS}: probability of greater difference between velocity dispersion distributions for groups with $b/a < 0.3$ and $b/a > 0.5$ occurring by chance (KS statistic).

argued that the probability that all three trends were present (albeit weak) was significant.[12]

Table 6 shows our analysis of the velocity dispersion and apparent elongations of the *quartets* (thus avoiding any geometrical source for the Tovmassian effect). In the *v2MCG* sample, there is no correlation between group apparent elongation and velocity dispersion, while in the cleaned HCG sample (Hick92/2) and the mock (from G11's SAM) CGs, there are weak correlations between σ_v and b/a, but they are not statistically significant. However, for the Hick92/2 and G11 samples, the median velocity dispersion of the chain-like ($b/a < 0.3$) groups is much smaller than that of the round ($b/a > 0.5$) groups, while the opposite behaviour is observed for the *v2MCG*s. Yet, the effect is not significant in the *v2MCG*, only marginally significant in the mock sample, while the Hick92/2 sample, with only 13 quartets, is too small to provide a statistically significant difference in the distributions of velocity dispersions between chain-like and round groups. We note that if we increase the Hick92/2 sample to groups with galaxy magnitudes $R < 14.97$ (instead of $R < 12.97$), we end up with 41 HCG quartets, for which the rank correlation coefficient between apparent elongation and velocity dispersion is now $r = 0.29$, yielding a correlation with 97 per cent significance. However, for this deeper Hick92/2 sample, the difference in the distributions of velocity dispersions for chain-like and round quartets is still not statistically significant.

6.2.4 *Bright end of the luminosity function*

Tremaine & Richstone (1977) devised two simple, yet powerful statistics, based on Cauchy–Schwarz inequalities, to test whether the first-ranked galaxies in groups and clusters were consistent with one or several arbitrary luminosity functions. They defined T_1 and T_2 as follows:

$$T_1 = \frac{\sigma(M_1)}{\langle M_2 - M_1\rangle} \quad T_2 = \frac{1}{\sqrt{0.677}}\,\frac{\sigma(M_2 - M_1)}{\langle M_2 - M_1\rangle}, \tag{3}$$

where the averages are means and where $\sigma(M_1)$ and $\sigma(M_2 - M_1)$ are the standard deviations of the absolute magnitude of the brightest galaxy (M_1) and difference in absolute magnitude ($M_2 - M_1$) between the second- and first-ranked galaxies, respectively. Values of T_1 and T_2 lower than unity imply that the first-ranked group galaxies are abnormally bright at the expense of the second-ranked galaxy. N-body simulations indicate that galaxy mergers within physically dense groups rapidly reduce the values of T_1 and T_2 below 0.7 (Mamon 1987a). T_1 and T_2 are biased low for samples with small number of groups, $N < 50$ (Mamon 1987b).

In Table 5, we find that the *v2MCG* sample displays T_1 and T_2 significantly lower than unity: $T_1 = 0.51 \pm 0.06$ and $T_2 = 0.70 \pm 0.06$ ($1\,\sigma$ errors from 10 000 bootstraps). We also find such low values in our mock *mvCG* sample from G11 as well as in our four other *mvCG* samples.

However, none of the other observed CG samples displays low values of T_1 and T_2. In particular, the HCG samples show $T_1 \approx 1.2$ and $\simeq T_2 \simeq 1.0$. It appears that Hickson (1982) missed CGs with very dominant galaxies (Prandoni et al. 1994; Díaz-Giménez & Mamon 2010), thus creating a spuriously high T_1. Indeed, Table 5 shows that $R_2 - R_1$ (hence the difference in absolute magnitudes) has a median value of 1.0 for the *v2MCG* sample (1.3 for the *mvCG*s), but only 0.6 for the HCG samples (the means are similar). Still, part of the difference in T_1 values is caused by the larger standard deviations of first-ranked absolute magnitudes in the HCG samples (0.8) in comparison with the *v2MCG* (0.53) and G11-*mvCG* (0.58) samples.

In comparison, Loh & Strauss (2006) found $T_1 = 0.75 \pm 0.1$ and $T_2 = 0.86 \pm 0.1$ in nearby rich SDSS clusters dominated by Luminous Red Galaxies (LRGs), while Lin, Ostriker & Miller (2010) recently found $T_1 = 0.70 \pm 0.01$ and $T_2 = 0.96 \pm 0.01$ in luminous SDSS clusters, but $T_1 = 0.84 \pm 0.01$ and $T_2 = 0.94 \pm 0.01$ for low luminosity ones.

We can also quantify how significant are the deviations of T_1 and T_2 from unity using a Monte Carlo technique (see also Lin et al. 2010). We built mock CGs by adopting the absolute magnitudes of the first-ranked *v2MCG*s and adding to them the absolute magnitudes of galaxies chosen at random from the 2MRS catalogue, but with three limitations: (1) in the same range of redshifts (velocities 1000 km s^{-1} from that of the first-ranked); (2) absolute magnitudes, M_K, in the range of the group: $M_K^{grp-1} \le M_K \le +M_K^{grp-1}+3$, where M_K^{grp-1} is the absolute magnitude of the first-ranked group member; (3) positions more than 5° from the group (in declination only for a faster run). The velocity criterion ensures that the flux limit of 2MRS is properly handled, while the position criterion ensures that a first-ranked galaxy is not duplicated in its mock group. In the end, we thus generate mock CGs with the same multiplicity function and distribution of most luminous absolute magnitudes. We did not consider a surface brightness threshold on our Monte Carlo groups (assuming that the galaxies are located in the same positions as in the observed sample), because this would increase the discrepancy between the observed values of T_1 and T_2 with those from our Monte Carlo samples. Indeed, since we start with the brightest group galaxy, if we enforced a minimum group surface brightness, we would tend to reject groups with only one luminous member, hence leading us to lower differences between second and first-ranked absolute magnitudes, and therefore larger values of T_1 and T_2. We compute T_1 and T_2 for this mock sample of CGs and iterate to build a total of 10 000 samples.

The distribution of T_1 and T_2 for the 10 000 mock catalogues can be seen in Fig. 6. Let p_i be the fraction of Monte Carlo realizations

[12] Tovmassian et al. (1999) did not present any statistical tests for the separate multiplicities, nor for the combination of the larger mean velocity dispersions for the triplets, quartets and quintets.

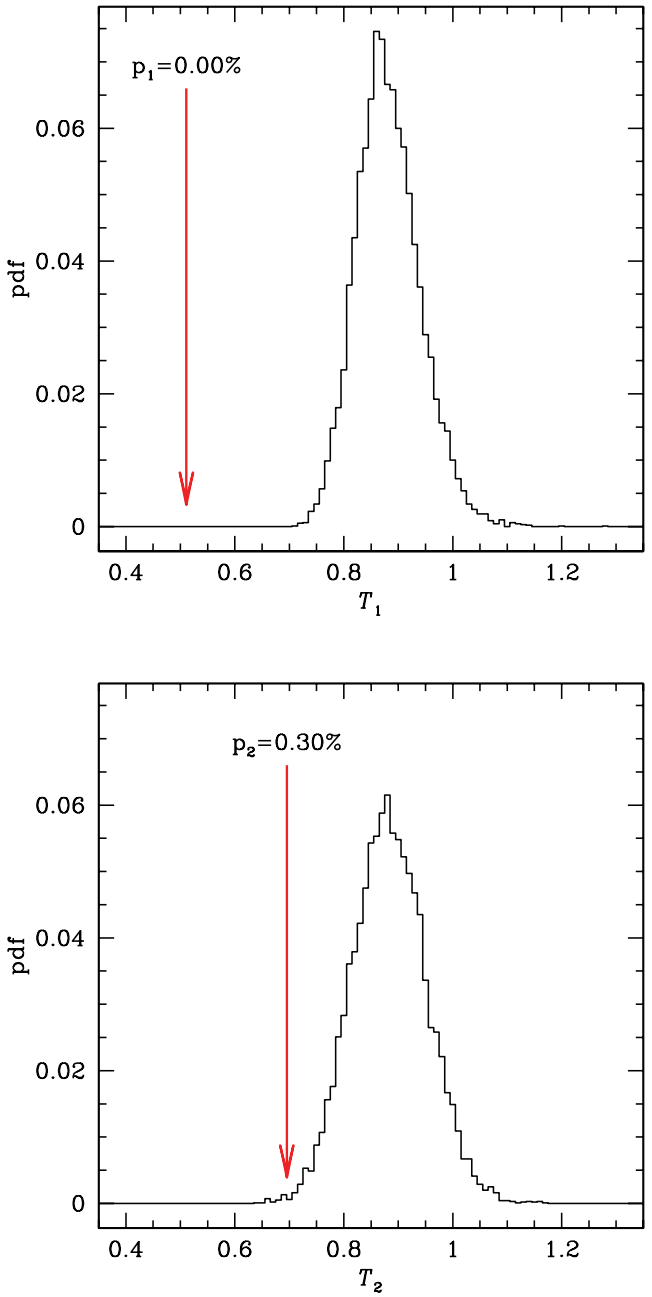

Figure 6. Distributions of Tremaine–Richstone statistics for 10 000 Monte Carlo realizations. *Vertical arrows* indicate the values observed in the *v2MCG* catalogue ($v > 3000\,\mathrm{km\,s^{-1}}$).

that have T_i as low as the observed value. We found $p_1 = 0$ (i.e. $p_1 < 0.01$ per cent) and $p_2 = 0.3 \pm 0.06$ per cent, i.e. none of our mocks reached values of T_1 and T_2 both as low as observed in *v2MCG*s.[13]

[13] Note that Lin et al. (2010) also considered the compatibility of the distribution of observed values of T_1 and T_2 of clusters using bootstrap resampling with the predicted distribution obtained with mocks. This incorrectly accounts twice for the finite sample. One should either use bootstraps to provide error bars on the observed T_1 and T_2 and compare to the mean prediction of the mocks or conversely compare the observed T_1 and T_2 without error bars to the distribution of the mocks, but not do both.

All this confirms that *the v2MCG is the only observed CG sample that has differences between first- and second-ranked absolute magnitudes that are inconsistent with random sampling of luminosity functions*, in agreement with the expectations from cosmological simulations.

6.2.5 *Luminosity segregation*

In the standard galaxy formation model used for SAMs, the brightest group galaxies are centrally located (see Skibba et al. 2011 for the quantification and limits of this idea). Indeed, *N*-body simulations of virialized dense groups show that such luminosity segregation rapidly sets in (Mamon 1987a). Moreover, the two-body relaxation times in dense groups of galaxies, of the order of the number of galaxies times the orbital time, both of which are small, are expected to be much smaller than the age of the Universe, hence galaxies should exchange their orbital energies and reach equipartition on short time-scales. If CGs are caused by chance alignments, then one does not expect to witness such luminosity segregation. Mamon (1986) measured luminosity segregation in HCGs, using exactly the same technique as he used in the simulations: stacking the groups and searching for a correlation (with the Spearman rank test) between the fraction of group luminosity in the galaxy (hereafter fractional luminosity) versus the projected distance relative to the group centroid (unweighted barycentre) in units of the median of these distances per group (hereafter normalized radial coordinate). The absence of luminosity segregation in HCGs, measured in this fashion, produced for him another argument that HCGs were heavily contaminated by chance alignments.

Here, we performed the same analysis on the different observed and mock samples of CGs. We first found that *v2MCG*s show significant anti-correlation between fractional luminosity and normalized distance: Spearman rank correlation $r = -0.19$. According to the Spearman rank correlation test, an anti-correlation at least as strong as this observed one has less than 0.1 per cent probability of arising by chance (see Table 5). This is also the case in the mock *mvCG* sample. One may argue that SAMs have luminosity segregation within them by construction, since in SAMs, galaxies form at the centre of a halo. But none of the other observed CG samples shows any significant sign of luminosity segregation, and this is not just a case of poorer statistics, as the correlation coefficient between fractional luminosities and normalized distances in the *v2MCG* is much more negative than in all other observed samples.

We also compared the stacked distributions of normalized distances between first- and second-ranked galaxies, as well as between second- and third-ranked galaxies, using the KS test. As seen in the last two rows in Table 5, in *v2MCG*s, the first-ranked galaxy is significantly more centrally located than the second-ranked galaxies: according to the KS test, the probability that this would occur by chance is again less than 0.1 per cent. This is also seen in the *mvCG*s, while no such significant trends are seen in the other group catalogues (including the HCG). Hence, *the v2MCG is the only CG sample to show that the most luminous galaxies are significantly more centrally located, in accordance with the mock CGs from SAMs, and contrary to what has been observed in all other CG sample.*

Interestingly, there are no statistically significant signs for different distributions of normalized distances between second- and third-ranked galaxies. In other words, while the first-ranked

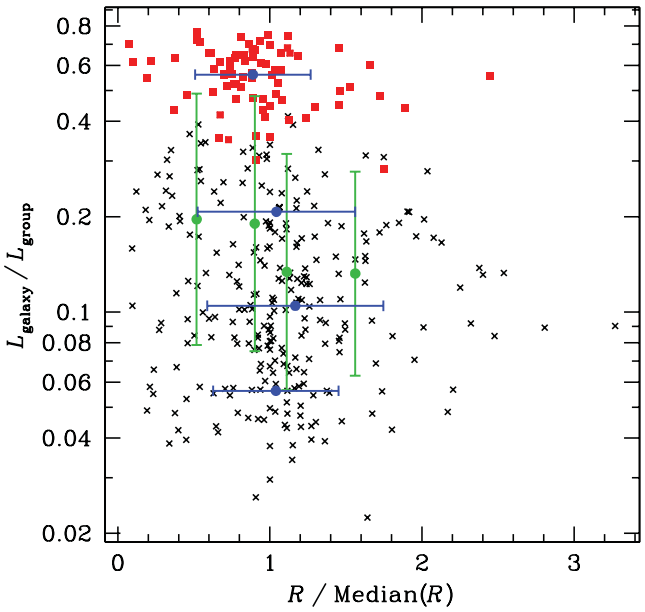

Figure 7. Luminosity segregation (fractional luminosity in group versus normalized radial coordinate relative to unweighted barycentre) in the *v2MCG* sample (restricted to $v > 3000\,\mathrm{km\,s^{-1}}$). The *red squares* indicate the first-ranked galaxies, while the *black crosses* show the other group galaxies. The *horizontal* and *vertical* error bars show the standard deviations in equal number subsamples of normalized radius and fractional luminosity, respectively. Despite the large scatter, the rank correlation coefficient is $r = -0.19$ and has only a probability of 3×10^{-4} of occurring by chance.

galaxies are in general more centrally located than the second-ranked, the latter are not more centrally located than the third-ranked. This lack of luminosity segregation among the non-brightest galaxies may occur because tides from the parent group potential may limit the sizes hence luminosities of the galaxies as they approach the central one (whose central location renders it immune to such tides). Then, the second most luminous galaxy will preferentially lie at the outskirts, while the third ranked one will tend to lie closer because of this tidal limitation. Therefore, for the non-brightest galaxies, group tides may cancel the effect of luminosity segregation.

Fig. 7 illustrates the luminosity segregation in the *v2MCG* sample. The fractional group luminosities appear to be enhanced within the median projected distance from the group centroid (i.e. abscissae smaller than unity). However, the normalized distances are only smaller in the galaxies in the 25 per cent highest quartile of fractional luminosity, which roughly corresponds to the first-ranked galaxies.

7 CONCLUSIONS AND DISCUSSION

In this work we have catalogued a new sample of CGs from the 2MASS survey and have compared them with existing CG samples.

Following the criteria defined by Hickson (1982), we have identified 230 CGs in projection in the *K*-band covering $23\,844\,\mathrm{deg^2}$. This catalogue has well-defined criteria which produced a homogeneous sample useful to perform statistical analyses on it. 25 per cent of them (57 CGs) were previously identified in other catalogues as CGs, triplets of galaxies or interacting galaxies. A total of 144 *p2MCG*s have *all* their members with redshifts available in the literature, and, among them, 85 groups have four or more accordant galaxies, which makes this catalogue the largest sample of CGs with four or more spectroscopically confirmed members. The percentage of groups with accordant galaxies (59 per cent) is slightly lower than that obtained from the HCG sample (67 per cent), and very similar to that predicted by Díaz-Giménez & Mamon (2010) from the SAMs of B06 and DLB07.[14]

As a side note, we have now built additional mock CG catalogues using the C06 SAM in the *K* band and the G11 SAM in the *r* band, where the latter was run on the Millennium-II Simulation, which has 512 times the mass resolution of the Millennium Simulation. For both samples, we found that two-thirds of the mock CGs were physically dense systems of at least four galaxies of accordant magnitudes, while the remaining third was caused by chance alignments of galaxies along the line of sight, mostly within larger virialized groups, confirming similar conclusions of Díaz-Giménez & Mamon (2010).

In comparison with other CG catalogues, the *v2MCG* catalogue presented in this work is one of the nearest and brightest samples of CGs, although these CGs have larger projected radii and interparticle separations.

The *v2MCG* does not show any significant correlation for quartets between apparent elongation and velocity dispersion nor significantly larger velocity dispersion in round groups relative to chain-like groups, contrary to what Tovmassian et al. (1999) claimed in HCGs.

The *v2MCG* is the only CG sample to display significantly large differences between second- and first-ranked absolute magnitudes (from Tremaine–Richstone statistics) as well as centrally located first-ranked galaxies, both in agreement with mock *mvCG*s, but in sharp contrast with all other observed velocity-filtered CG samples.

Galaxy mergers are an obvious way to decrease T_1 and T_2 (Mamon 1987a), and we cannot think of any other physical mechanism that may cause both T_1 and T_2 to be significantly smaller than unity in a group catalogue.

One major difference of our sample with others is that ours has many more groups with dominant galaxies accounting for over half the total luminosity. While this increases the gap between first- and second-ranked magnitudes, we found that our sample also has a small standard deviation of first-ranked absolute magnitudes, which enhances the significance of the Tremaine–Richstone T_1 statistic.

Why do not we find significant magnitude gaps and luminosity segregation in the other CG samples? It is clear that in his visual search for CGs, Hickson (1982) missed groups with dominant galaxies (Prandoni et al. 1994; Díaz-Giménez & Mamon 2010 and Table 5). Could those *v2MCG*s in common with *vHCG*s have weaker signs of magnitude gaps and luminosity segregation? One expects that if mergers cause the magnitude gap, the masses, i.e. stellar masses, of the galaxies are the crucial variable. Similarly, if luminosity segregation is produced by dynamical friction or by energy equipartition from two-body relaxation, the galaxy (stellar) masses should be the important variable. Therefore, the magnitude gaps and luminosity segregation should be weaker in the *R* band, where the luminosity is less a measure of stellar mass than in the *K* band.

Unfortunately, we have only 14 groups in common, among which 10 (HCG 7, 10, 23, 25, 40, 58, 86, 88, 93, 99)[15] have exactly the same galaxies. For these 10 groups, we find $T_1 = 0.68 \pm 0.24$ and $T_2 = 0.87 \pm 0.24$ in the *K* band, while in the *R* band we find values

[14] For the SAM of G11, we find that 70 per cent of mock CGs found in projected space survive the velocity filtering.
[15] With slight variations: HCG 15, 16, 51, 97.

greater than unity: $T_1 = 1.75 \pm 1.69$ and $T_2 = 1.33 \pm 0.39$. So, indeed, the *K*-band luminosities are more sensitive than their *R*-band counterparts to the magnitude gap, but given the bootstrap errors, the large differences in T_1 and T_2 between *R*- and *K*-based absolute magnitudes are not statistically significant (for T_2 the difference is roughly 1σ, while it is much less for T_1). On the other hand, luminosity segregation is not seen in either waveband: worse it is inverted, with the brightest galaxy on average further away from the group centroid than the second-brightest galaxy.

The other two CG samples, UZC-CG and LCCG, are based upon Friends-of-Friends (LCCG) or similar (UZC-CG) algorithms, both with velocity linking length of $1000\,\mathrm{km\,s^{-1}}$. Such a velocity link is much more liberal than imposing that the velocities all lie within $1000\,\mathrm{km\,s^{-1}}$ from the median as done in Hickson et al. (1992) and here. Indeed, according to Table 5, the median velocity dispersion of UZC-CG groups of four or more galaxies is $295\,\mathrm{km\,s^{-1}}$, i.e. 25 per cent greater than in our sample. This suggests that the UZC-CG sample is more contaminated by chance alignments of galaxies along the line of sight (as Mamon 1986 had suggested for the HCG sample) than is our sample. Moreover, the UZC-CG has a liberal linking length on projected distances of $200\,h^{-1}$ kpc, making these groups not so compact (as can be checked by their low mean group surface brightness as seen in Table 5). Finally, the UZC-CG is based upon Zwicky's visually estimated magnitudes, which may carry rms errors as large as 0.5 mag, thus washing out in part the effects of the magnitude gap and luminosity segregation.

On the other hand, the LCCG sample (again, restricted to groups with at least four members) has a very similar median velocity dispersion to our sample (and a similar median mass-to-light ratio). Note that the linking length for projected distances of the LCCG is only $50\,h^{-1}$ kpc, i.e. four times less than in UZC-CG. The problem with the LCCG is that its parent catalogue (the LCRS; Shectman et al. 1996) is a collection of two samples with $16.0 < R < 17.3$ and $15.0 < R < 17.7$. Thus, the magnitude range is very restricted. Hence, it is not a surprise that $\langle M_2 - M_1 \rangle$ is half our value (Table 5), leading to $T_1 > 1$ and $T_2 > 1$.

What does this tell us on the nature of the groups in the different CG samples? Over 25 years ago, Mamon (1986) found $T_1 = 1.16$ and no signs of luminosity segregation in the largest sample then available of 41 velocity-filtered HCGs with at least four members. This was in sharp contrast with the low values of T_1 and significant luminosity segregation he was finding in coalescing dense groups (Mamon 1987a). This provided him with two arguments (among several) to conclude that most HCGs were caused by chance alignments of galaxies within larger groups (Mamon 1986). As confirmed here with the SAM by G11, roughly two-thirds of mock CGs are physically dense (Díaz-Giménez & Mamon 2010 and Table 3). The statistically large magnitude gaps and luminosity segregation in both the observed *v2MCG*s and the mock *mvCG*s suggest that Mamon (1986) was misled by the bias of the HCG sample against large gaps into concluding that most of them were not physically dense.

So the *v2MCG* appears to be mostly *bona fide* physically dense groups. But can we conclude that the other CG samples are dominated by chance alignments? Díaz-Giménez & Mamon (2010) attempted to build a sample of mock HCGs that include the same biases as they had measured by comparing with the three SAMs that they had built mock CGs from. They found that the same fraction (if not slightly higher) of the mock (biased) HCGs were physically dense. The nature of the groups in other CG samples could be studied in similar ways, using mock CG samples from cosmological galaxy formation simulations, mimicking their selection criteria and observational select effects.

Table 7. Luminosity segregation split by magnitude gap.

Catalogue	Subsample	N	$P_{\rm KS}$
v2MCG	Dom	39	2.9×10^{-7}
v2MCG	Non-Dom	39	(3.9 per cent)
vHCG	Dom	17	67 per cent
vHCG	Non-Dom	16	(6.6 per cent)
mvCG-G11	Dom	163	1.2×10^{-11}
mvCG-G11	Non-Dom	163	1.0 per cent
mvCG-C06K	Dom	223	4.0×10^{-9}
mvCG-C06K	Non-Dom	225	0.4 per cent

Note. Dom and Non-Dom subsamples are those with $M_2 - M_1$ above and below the median value of the full sample, respectively. N is the number of groups in the subsample. $P_{\rm KS}$ is the KS probability that a difference in the distributions of normalized distances to the non-weighted group centre is greater than 'observed' by chance. Values of $P_{\rm KS}$ given in parentheses denote reverse luminosity segregation: the second-ranked galaxy is more centrally located than the first ranked.

Could the lack of HCGs with strongly dominant brightest galaxies prevent the visibility of luminosity segregation? We performed KS tests to compare the distribution of relative positions of first- and second-ranked group members for subsamples split between those dominated by first-ranked members ('Dom') and those with galaxies of more comparable luminosities ('Non-Dom'), making our splits at the median magnitude difference $\langle M_2 - M_1 \rangle$. We performed this analysis for the HCG and *v2MCG* samples as well as for the C06K and G11 *mvCG* samples. Table 7 shows that, indeed, luminosity segregation is much stronger for all catalogues in the Dom subsamples, and statistically significant in all of them except the *vHCG*. Surprisingly, while the Non-Dom subsamples of the two mock CG samples display much weaker, but still statistically significant, luminosity segregation, the Non-Dom subsamples of both the *v2MCG* and *vHCG* catalogues display *reversed luminosity segregation*: the second-ranked galaxy is more centrally located than the (slightly more luminous) first-ranked galaxy. We can only see one explanation for this reverse luminosity segregation, if it occurs in wavebands bluer than *K*: late-type galaxies that are second-ranked in stellar mass, hence not centrally located, can end up more luminous (thanks to their efficient star formation) than early-type galaxies of slightly higher stellar mass. However, the effect is also present in the *K*-selected *v2MCG*, and with even greater statistical significance (96.1 versus 93.7 per cent confidence for the Non-Dom CGs of the *v2MCG* and *vHCG* catalogues, respectively). So, we can only explain this marginal effect as a statistical fluke.

Nevertheless, the absence of luminosity segregation in the HCG catalogue could be consistent with their physical reality because the sample is too small to detect the weak luminosity segregation expected from the mocks. Moreover, if the reverse luminosity segregation for Non-Dom groups is real, then the lack of groups with very dominant galaxies in the HCG (caused by the visual selection bias) would cause the Non-Dom groups to cancel the luminosity segregation of the Dom groups.

In conclusion, the *v2MCG* sample has numerous advantages over other CG samples:

(i) It is the largest available sample of velocity-filtered groups of at least four members of comparable luminosity (3 mag, i.e. a factor of 16).

(ii) It has an isolation criterion (in contrast with other CG samples except for the HCG).

(iii) It is automatically extracted (contrary to the HCG).

(iv) It has a well-defined magnitude limit (which the HCG sample does not).

(v) It is deep enough (which some may find surprising given the shallowness of its parent 2MASS catalogue) to have a selection on brightest galaxy magnitude, so as to ensure that all groups can span the maximum allowed magnitude gap of 3.

(vi) It is selected by stellar mass (K band), which is expected to be a better tracer for magnitude gaps and luminosity segregation (among other things).

(vii) It is the only sample to show statistical signs of mergers (magnitude gaps) and luminosity segregation, expected in physically dense groups (in contrast with all other CG samples).

The last point implies that the *v2MCG* is the only CG sample for which one is reasonably sure that it is dominated by physically dense groups. For all these reasons, the *v2MCG* appears to be the sample one ought to study in depth to probe the effects on galaxies of this unique environment of four galaxies of comparable luminosity lying close together in real space.

As a next step in this project, we are in the process of measuring redshifts for the members for which no spectra are available, and we are continuing our statistical studies of the *v2MCG*s and their galaxies.

ACKNOWLEDGMENTS

We thank the anonymous referee for helpful comments that improved this work.

We dedicate this article to John P. Huchra (1948–2010), who among his numerous contributions to astronomy played a crucial role in obtaining redshifts for the galaxies in groups in general and HCGs in particular. We thank Roya Mohayaee and Guilhem Lavaux for useful discussions on peculiar velocities and Igor Chilingarian on k-corrections and internal extinctions.

This publication makes use of data products from the 2MASS, which is a joint project of the University of Massachusetts and the Infrared Processing and Analysis Centre/California Institute of Technology, funded by the National Aeronautics and Space Administration and the National Science Foundation. This research has made use of VizieR and Aladin at the Centre de Données astronomiques de Strasbourg (CDS). This research made use of the 'K-corrections calculator' service available at http://kcor.sai.msu.ru/. An SM version (`kcorr_Chilingarian`) is available at ftp://ftp.iap.fr/from_users/gam/SOFT/gam_macros. The Millennium and Millennium II Simulation data bases used in this paper and the web application providing online access to them were constructed as part of the activities of the German Astrophysical Virtual Observatory. This work was partially supported by Consejo de Investigaciones Científicas y Técnicas de la República Argentina (CONICET) and Fundação de Amparo à Pesquisa do Estado do São Paulo (FAPESP). CMdO acknowledges financial support from FAPESP and CNPq.

REFERENCES

Allam S. S., Tucker D. L., 2000, Astron. Nachr., 321, 101
Arp H., 1966, ApJS, 14, 1
Arp H. C., Madore B. F., 1987, in Arp H. C., Madore B. F., eds, A Catalogue of Southern Peculiar Galaxies and Associations. Cambridge Univ. Press, Cambridge
Barnes J., 1985, MNRAS, 215, 517
Barton E., Geller M., Ramella M., Marzke R. O., da Costa L. N., 1996, AJ, 112, 871
Beers T. C., Flynn K., Gebhardt K., 1990, AJ, 100, 32
Binney J., Tremaine S., 1987, Galactic Dynamics. Princeton Univ. Press, Princeton, NJ,
Bode P. W., Cohn H. N., Lugger P. M., 1993, ApJ, 416, 17
Bonnarel F. et al., 2000, A&AS, 143, 33
Borthakur S., Yun M. S., Verdes-Montenegro L., 2010, ApJ, 710, 385
Bower R. G., Benson A. J., Malbon R., Helly J. C., Frenk C. S., Baugh C. M., Cole S., Lacey C. G., 2006, MNRAS, 370, 645 (B06)
Boylan-Kolchin M., Springel V., White S. D. M., Jenkins A., Lemson G., 2009, MNRAS, 398, 1150
Cardelli J. A., Clayton G. C., Mathis J. S., 1989, ApJ, 345, 245
Carnevali P., Cavaliere A., Santangelo P., 1981, ApJ, 249, 449
Chilingarian I. V., Melchior A.-L., Zolotukhin I. Y., 2010, MNRAS, 405, 1409
Coziol R., Ribeiro A. L. B., de Carvalho R. R., Capelato H. V., 1998, ApJ, 493, 563
Crook A. C., Huchra J. P., Martimbeau N., Masters K. L., Jarrett T., Macri L. M., 2008, ApJ, 685, 1320
Croton D. J. et al., 2006, MNRAS, 365, 11 (C06)
de Carvalho R. R., Gonçalves T. S., Iovino A., Kohl-Moreira J. L., Gal R. R., Djorgovski S. G., 2005, AJ, 130, 425
de la Rosa I. G., de Carvalho R. R., Zepf S. E., 2001, AJ, 122, 93
de la Rosa I. G., de Carvalho R. R., Vazdekis A., Barbuy B., 2007, AJ, 133, 330
De Lucia G., Blaizot J., 2007, MNRAS, 375, 2 (DLB07)
Deng X.-F., He J.-Z., Ma X.-S., Jiang P., Tang X.-X., 2008, Central Eur. J. Phys., 6, 185
Díaz-Giménez E., Mamon G., 2010, MNRAS, 409, 1227
Focardi P., Kelm B., 2002, A&A, 391, 35
Górski K. M., Hivon E., Banday A. J., Wandelt B. D., Hansen F. K., Reinecke M., Bartelmann M., 2005, ApJ, 622, 759
Guo Q. et al., 2011, MNRAS, 413, 101 (G11)
Hickson P., 1982, ApJ, 255, 382
Hickson P., Ninkov Z., Huchra J., Mamon G., 1984, in Mardirossian F., Giuricin G., Mezzetti M., eds, Clusters and Groups of Galaxies. Reidel, Dordrecht, p. 367
Hickson P., Kindl E., Auman J. R., 1989, ApJS, 7, 687
Hickson P., Mendes de Oliveira C., Huchra J. P., Palumbo G. G., 1992, ApJ, 399, 353
Huchra J. P. et al., 2012, ApJS, 199, 26
Iovino A., 2002, AJ, 124, 2471
Iovino A., de Carvalho R., Gal R., Odewahn S., Lopes P., Mahabal A., Djorgovski S., 2003, AJ, 125, 1660
Jarrett T. H., Chester T., Cutri R., Schneider S., Skrutskie M., Huchra J. P., 2000, AJ, 119, 2498
Karachentsev I. D., 1972, Astrofizicheskie Issledovaniia Izvestiya Spetsial'noj Astrofizicheskoj Observatorii, 7, 3
Karachentsev V. E., Karachentsev I. D., Lebedev V. S., 1988, Astrofizicheskie Issledovaniia Izvestiya Spetsial'noj Astrofizicheskoj Observatorii, 26, 42
Karachentseva V. E., Karachentsev I. D., 2000, Astron. Rep., 44, 501
Lavaux G., Hudson M. J., 2011, MNRAS, 416, 2840
Lavaux G., Tully R. B., Mohayaee R., Colombi S., 2010, ApJ, 709, 483
Lee B. C. et al., 2004, AJ, 127, 1811
Lin Y.-T., Ostriker J. P., Miller C. J., 2010, ApJ, 715, 1486
Loh Y.-S., Strauss M. A., 2006, MNRAS, 366, 373
McConnachie A. W., Patton D. R., Ellison S. L., Simard L., 2009, MNRAS, 395, 255
Maller A. H., McIntosh D. H., Katz N., Weinberg M. D., 2005, ApJ, 619, 147
Mamon G. A., 1986, ApJ, 307, 426
Mamon G. A., 1987a, ApJ, 321, 622
Mamon G. A., 1987b, BAAS, 19, 651
Mamon G. A., 1989, A&A, 219, 98
Mamon G. A., 1992, ApJ, 401, L3

Mamon G. A., 1994, Ap&SS, 217, 237
Mamon G. A., 2008, A&A, 486, 113
Masters K. L., Giovanelli R., Haynes M. P., 2003, AJ, 126, 158
Mendes de Oliveira C., Hickson P., 1991, ApJ, 380, 30
Moles M., del Olmo A., Perea J., Masegosa J., Marquez I., Costa V., 1994, A&A, 285, 404
Mould J. R. et al., 2000, ApJ, 529, 786
Poggianti B. M., 1997, A&A, 122, 399
Pompei E., Iovino A., 2012, A&A, 539, A106
Ponman T. J., Bourner P. D. J., Ebeling H., Böhringer H., 1996, MNRAS, 283, 690
Prandoni I., Iovino A., MacGillivray H. T., 1994, AJ, 107, 1235
Ramella M., Geller M. J., Pisani A., da Costa L. N., 2002, AJ, 123, 2976
Rose J. A., 1977, ApJ, 211, 311
Schlegel D. J., Finkbeiner D. P., Davis M., 1998, ApJ, 500, 525
Seyfert C. K., 1948, AJ, 53, 203
Shectman S. A., Landy S. D., Oemler A., Tucker D. L., Lin H., Kirshner R. P., Schechter P. L., 1996, ApJ, 470, 172
Skibba R. A., van den Bosch F. C., Yang X., More S., Mo H., Fontanot F., 2011, MNRAS, 410, 417
Skrutskie M. F. et al., 2006, AJ, 131, 1163
Springel V. et al., 2005, Nat, 435, 629
Stephan M., 1877, MNRAS, 37, 334
Sulentic J. W., 1997, ApJ, 482, 640
Terry J. N., Paturel G., Ekholm T., 2002, A&A, 393, 57
Torres-Flores S., Mendes de Oliveira C., Amram P., Plana H., Epinat B., Carignan C., Balkowski C., 2010, A&A, 521, 59
Tovmassian H. M., Martinez O., Tiersch H., 1999, A&A, 348, 693
Tremaine S. D., Richstone D. O., 1977, ApJ, 212, 311
Tzanavaris P. et al., 2010, ApJ, 716, 556
Verdes-Montenegro L., Yun M. S., Williams B. A., Huchtmeier W. K., Del Olmo A., Perea J., 2001, A&A, 377, 812
Vorontsov-Velyaminov B. A., Noskova R. I., Arkhipova V. P., 2001, Astron. Astrophys. Trans., 20, 717
Wainer H., Thissen D., 1976, Psychometrica, 41, 9
Walke D. G., Mamon G. A., 1989, A&A, 225, 291
White R. A., Bliton M., Bhavsar S. P., Bornmann P., Burns J. O., Ledlow M. J., Loken C., 1999, AJ, 118, 2014

APPENDIX A: TRANSFORMATION FROM μ_R TO μ_K

In the visual search performed by Hickson (1982) on the photographic plates of POSS-I, he established a cut-off in surface brightness of $\mu_E = 26\,\mathrm{mag\,arcsec^{-2}}$. The POSS-I E band roughly corresponds to the more familiar Cousins R band. As the galaxy data base used for our search is selected in the K_s band, we converted the original limit of Hickson (1982) to a corresponding one for K magnitudes. The $R - K$ colours[16] of galaxies depend on their luminosity (colour–luminosity relation) and morphology (e.g. Red Sequence versus Blue Cloud).

We cross-identified the SDSS DR7 model g and r magnitudes, A_g and A_r extinctions, and redshifts with the 2MASS XSC $K20$ isophotal J and K magnitudes, with a maximum separation of 2 arcsec between the positions of the galaxies in the two catalogues. We corrected the 2MASS magnitudes for galactic extinction using the A_g values of the SDSS, assuming $A_g/A_V = 1.256$, $A_r/A_V = 0.798$ and $A_{K_s}/A_V = 1.16$ from spline fits of $\log A_\lambda$ versus $\log\lambda$ tabulated by Cardelli, Clayton & Mathis (1989) and $A_J/A_V = 0.282$ directly from their table. We then k-corrected the SDSS r and 2MASS K_s extinction-corrected magnitudes using the redshifts and extinction-corrected $g - r$ (SDSS) and the $J - K_s$ (2MASS) colours using the transformations of Chilingarian et al. (2010). This enabled us to derive extinction- and k-corrected $(r - K)^0$ colours.

In a first pass, we adopt the conservative $(r - K)^0 = 2.33$, which, with $(r - R)^0 = 0.33$ (Díaz-Giménez & Mamon 2010), yields $\mu_K \leq 24\,\mathrm{mag\,arcsec^{-2}}$. Once we extract the *p2MCG*s and then the velocity-filtered *v2MCG*s with this compactness limit, we find that the mean galaxy luminosity in our *v2MCG*s is $M_K = -23.40 + 5\log h$ and our median *v2MCG* mean velocity is $5927\,\mathrm{km\,s^{-1}}$, corresponding to $z = 0.020$. In a second pass, we consider the $(r - K)^0$ colours for the 45974 galaxies among the 326320 SDSS–2MASS matches, with SDSS `zWarn` $= 0$, $13 < r < 17.77$, and 2MASS artefact flag `cc_flg` $= 0$ and both J and K confusion flags, respectively, `j_flg_k20fe` and `k_flg_k20fe`, equal to 0 (grey points of Fig. A1). Restricting these matched galaxies to those with $M_K - 5\log h = -23.40 \pm 0.10$ and $z = 0.020 \pm 0.005$ (large blue points in Fig. A1) yields a median $(r - K)^0$ of 2.72 ± 0.04 (assuming that the error on the median is $1.253\,\sigma/\sqrt{N}$, valid for large Gaussian distributions) for 164 galaxies.

With $(r - R)^0 = 0.33$, this yields $(R - K)^0 = 2.39$. For clarity, we therefore assume $R = K + 2.4$ and adopt a compactness limit of $\mu_K = 23.6$. The *v2MCG*s obtained with this new compactness limit have very similar median redshifts (now 1.5 per cent larger), although the median R-band group luminosities are now one-third lower (mainly because of the additional 0.4 mag correction from K to R).

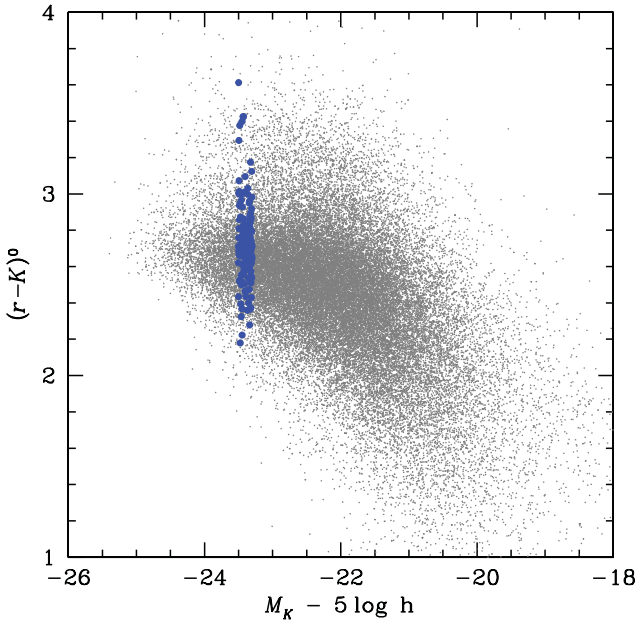

Figure A1. Colour–luminosity relation for SDSS–2MASS matches. The *grey points* show all 45 974 non-flagged galaxies with $0.005 < z < 0.05$, $13 < r < 17.77$, $K < 13.57$, while the *blue points* use the additional criteria $M_K - 5\log h = -23.40 \pm 0.10$ and $z = 0.020 \pm 0.005$.

APPENDIX B: COMPARISON WITH DIFFERENT SAMS

In Fig. 5, we showed the comparison of the distributions of velocity-filtered CG properties between the *v2MCG* and the *mvCG* (from G11 run on the MS-II) samples. In Fig. B1, we show this comparison

[16] We drop the 's' subscript on the K_s band for clarity.

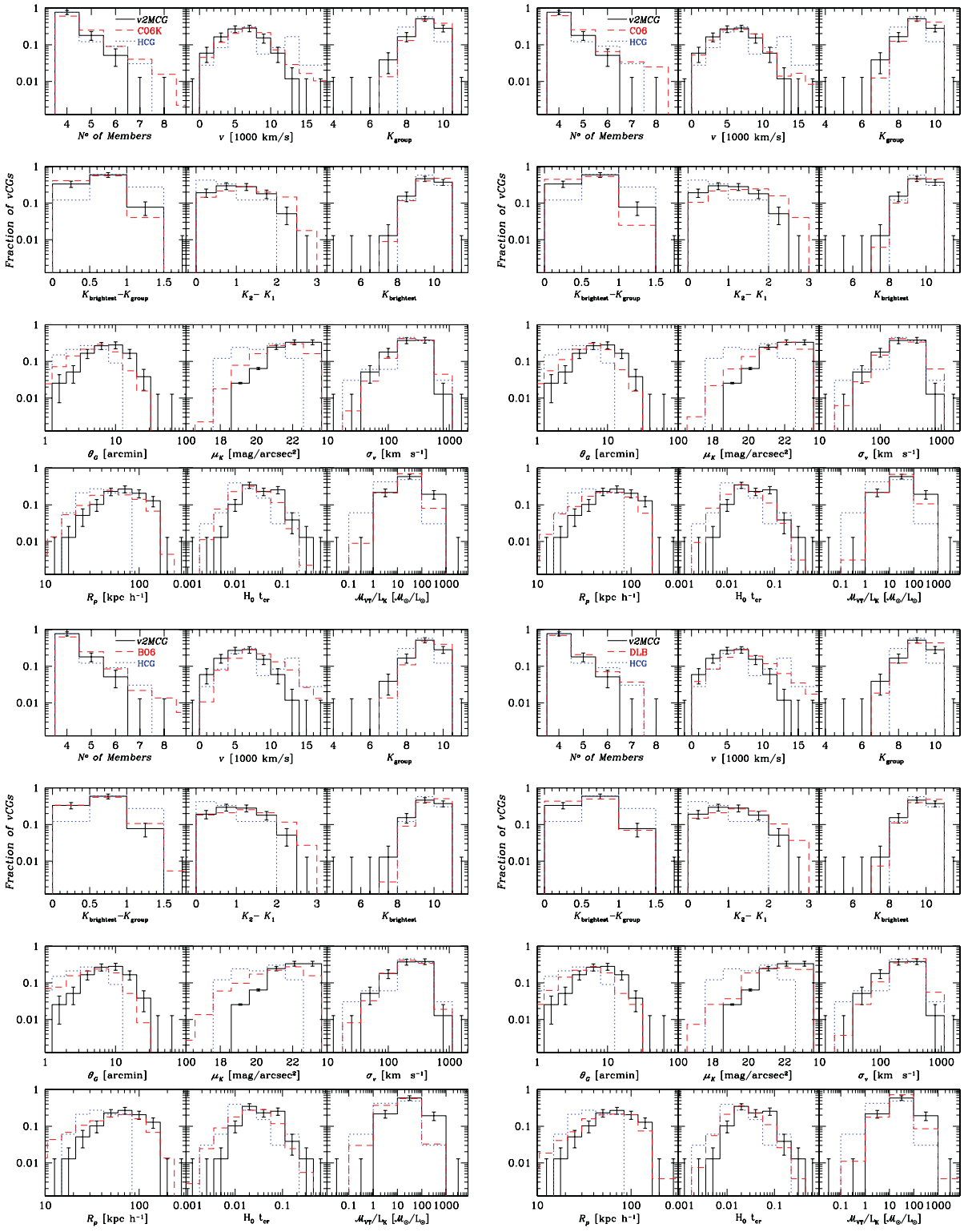

Figure B1. Distribution of properties of the *v2MCG* (*solid lines*) and HCG92/2 (*dotted lines*) samples, compared with different SAMs (*dashed lines*). Error bars correspond to Poisson errors.

for several SAMs: left-upper panels: *mvCG*s identified from C06's SAM in the *K* band; right-upper panels: *mvCG*s identified from C06's SAM in the *R* band; left-lower panels: *mvCG*s identified from B06's SAM in the *R* band; right-lower panels: *mvCG*s identified from DLB07's SAM in the *R* band.

APPENDIX C: PROPERTIES OF CGS AFTER VELOCITY-FILTERING IN THE 2MASS XSC

Table C1. CGs after velocity filtering in the 2MASS XSC.

ID	RA (J2000)	Dec. (J2000)	v (km s^{-1})	N	K_b	μ_K (mag arcsec^{-2})	θ_G (arcmin)	$\langle R_{ij}\rangle$ (kpc h^{-1})	b/a	σ_v (km s^{-1})	$H_0\,t_{cr}$	M_{VT}/L_K ($h\,\mathcal{M}_\odot/L_\odot$)	cross-ID
1	00:00:43	28:23:18	8705	5	10.41	19.92	2.34	43.44	0.67	322	0.012	28	HCG 99, KTG 83,VV 854
2	00:00:59	−43:22:47	11 525	4	10.14	22.23	6.07	121.73	0.30	479	0.023	148	···
3	00:28:54	02:45:34	4241	5	8.58	23.18	18.04	50.06	0.08	175	0.026	11	UZC-CG 7, VV 894
4	00:39:24	00:52:28	4209	4	9.33	21.00	5.58	45.56	0.53	130	0.032	10	HCG 7, UZC-CG 9, USGC U024
5	00:56:42	−52:56:40	7561	4	9.50	21.29	5.71	92.15	0.37	534	0.016	108	···
6	00:57:48	−05:02:22	5345	6	10.20	22.81	11.38	85.80	0.46	294	0.026	90	···
7	01:08:58	−45:48:11	7598	4	9.87	21.05	4.18	44.85	0.11	291	0.014	29	···
8	01:13:55	−31:48:02	5687	4	8.79	21.15	7.30	85.77	0.78	293	0.027	39	SCG 1
9	01:26:05	34:41:39	4742	4	9.21	22.08	10.63	92.15	0.41	257	0.032	44	HCG 10, RSCG 12
10	01:43:24	−34:14:40	3786	4	10.11	23.20	11.09	62.52	0.24	149	0.038	46	SCG 0141-3429
11	02:07:39	02:08:30	7042	4	10.40	22.57	7.60	89.13	0.40	443	0.018	226	HCG 15
12	02:09:49	−10:13:37	3874	5	9.04	22.82	17.94	63.75	0.12	147	0.039	10	HCG 16, USGC S077, RSCG 19, VV 1007
13	02:36:55	07:22:28	6310	4	9.48	23.38	14.37	168.32	0.50	325	0.047	110	USGC U136
14	02:42:05	−15:04:36	7437	4	10.57	21.03	3.59	53.33	0.29	73	0.066	3	SCG 19, USGC S093
15	02:45:07	−17:42:28	7412	4	9.75	22.91	13.61	164.29	0.28	218	0.068	38	HCG 21
16	03:03:50	−12:02:25	3648	4	8.73	21.52	8.45	67.71	0.32	396	0.016	122	SCG 3
17	03:07:05	−09:35:15	4851	4	9.87	21.75	7.04	65.73	0.69	330	0.018	106	HCG 23, SCG 11
18	03:07:29	−66:48:22	5580	4	9.55	23.48	16.76	194.28	0.74	174	0.101	61	SCG 0306-6659
19	03:17:44	−10:19:56	8882	4	10.06	22.58	6.97	103.54	0.35	440	0.021	135	···
20	03:20:40	−01:04:18	6288	4	10.52	21.87	4.55	47.93	0.40	87	0.050	6	HCG 25
21	03:25:22	−06:09:30	10335	4	10.44	22.12	5.85	116.75	0.36	157	0.067	17	···
22	03:46:31	−04:12:39	3917	5	8.18	23.38	29.15	140.46	0.40	145	0.088	15	···
23	04:51:45	−03:52:38	4633	4	10.14	22.83	8.34	74.54	0.57	83	0.082	13	···
24	04:59:25	−11:08:00	3823	6	9.03	22.60	18.32	99.91	0.56	357	0.025	59	KTS 28, VV 699
25	06:03:55	−32:06:38	9565	4	10.09	23.16	9.23	129.26	0.10	460	0.026	73	···
26	06:43:41	−74:14:45	6458	4	9.54	21.37	6.09	59.98	0.23	377	0.014	58	VV 785
27	07:04:34	64:03:45	4468	4	9.55	22.99	11.27	94.36	0.25	66	0.129	8	···
28	07:26:32	85:37:41	2177	4	7.74	22.71	22.30	83.25	0.46	262	0.029	98	VV 1189
29	07:40:56	55:25:55	10752	4	9.90	19.38	1.73	32.21	0.42	436	0.007	32	···
30	09:05:05	18:21:41	4188	5	9.01	23.51	17.54	142.04	0.79	391	0.033	317	VV 612
31	09:16:30	30:52:02	6954	4	9.82	22.64	8.38	85.16	0.11	73	0.106	3	···
32	09:27:57	30:00:35	7994	4	10.24	21.21	3.56	48.52	0.64	387	0.011	106	···
33	09:34:23	10:09:24	3141	4	8.86	23.29	19.19	105.31	0.37	355	0.027	207	RSCG 33, VV 1290/1292
34	09:38:55	−04:51:05	6633	5	9.73	18.60	1.74	15.19	0.36	189	0.007	4	HCG 40, VV 116
35	10:00:01	−19:34:37	4020	4	8.18	22.74	18.18	105.27	0.08	119	0.081	6	HCG 42
36	10:25:07	28:03:09	6361	4	10.14	21.84	5.07	72.55	0.84	188	0.035	47	···
37	10:37:15	−26:14:56	3433	4	9.29	22.59	10.66	79.84	0.59	268	0.027	142	···
38	10:39:43	−23:49:47	3758	4	9.97	23.32	11.88	100.45	0.95	159	0.057	71	···
39	10:51:52	50:56:02	7491	5	10.08	23.14	11.22	139.23	0.46	497	0.025	78	VV 1393
40	11:09:46	21:46:22	9552	4	10.01	21.52	4.81	64.52	0.08	103	0.057	3	···
41	11:16:12	18:07:46	896	4	7.11	21.95	21.98	36.44	0.33	289	0.011	98	···
42	11:22:21	24:18:31	7619	4	10.07	21.12	4.07	63.83	0.20	322	0.018	46	HCG 51, UZC-CG 138, VV 1435
43	11:35:11	51:12:03	8010	4	10.41	21.94	4.76	57.86	0.44	325	0.016	102	···
44	11:42:10	10:18:52	6218	5	9.63	21.86	8.82	91.33	0.60	173	0.048	17	HCG 58, UZC-CG 144
45	11:42:51	26:31:54	9054	4	10.06	22.87	9.91	126.33	0.11	355	0.032	68	···
46	11:44:06	33:30:45	9381	4	10.16	21.25	3.78	67.96	0.43	144	0.043	8	···
47	11:57:06	55:17:50	948	4	7.42	22.44	23.41	51.99	0.45	211	0.022	88	···
48	12:19:22	05:57:42	2156	4	7.40	21.67	16.44	73.71	0.39	348	0.019	89	···
49	12:24:31	07:09:38	994	5	6.79	22.83	36.02	64.63	0.46	215	0.027	91	···
50	12:27:47	12:11:30	1024	4	8.99	23.12	15.53	28.03	0.32	557	0.005	1560	···
51	12:43:17	11:25:08	1117	5	5.81	22.16	45.77	75.83	0.38	363	0.019	56	M60 CG, VV 206/1558
52	13:01:58	27:37:34	7473	4	10.03	21.90	5.07	61.27	0.21	704	0.008	401	···
53	13:06:50	−40:22:49	4768	4	8.83	22.20	10.29	118.12	0.55	116	0.092	14	HDCE 0761
54	13:08:15	34:01:53	10120	4	10.50	23.41	10.77	180.87	0.54	185	0.089	47	···
55	13:22:02	−17:21:16	6909	5	9.95	22.11	6.15	71.02	0.44	241	0.027	50	···
56	13:24:31	14:01:36	7087	4	9.37	22.75	11.94	177.44	0.47	278	0.058	76	···
57	13:52:16	02:20:05	7095	4	9.80	20.74	3.42	51.30	0.52	50	0.094	1	···
58	13:53:01	−28:27:48	4713	5	8.54	21.08	7.27	43.75	0.13	261	0.015	20	···
59	14:00:33	−02:51:35	7325	6	9.82	21.73	6.12	60.26	0.31	322	0.017	37	···
60	14:19:14	35:08:15	8534	4	10.34	22.52	6.12	74.71	0.28	52	0.131	3	···
61	14:27:27	11:19:18	8078	4	10.45	22.51	6.47	108.69	0.70	424	0.023	245	···
62	14:28:02	25:53:33	4388	4	9.33	21.86	8.31	67.15	0.58	216	0.028	42	···

Table C1 – *continued*

ID	RA	Dec. (J2000)	v (km s^{-1})	N	K_b	μ_K (mag arcsec^{-2})	θ_G (arcmin)	$\langle R_{ij}\rangle$ (kpc h^{-1})	b/a	σ_v (km s^{-1})	$H_0\,t_{cr}$	M_{VT}/L_K ($h\,\mathcal{M}_\odot/L_\odot$)	cross-ID
63	14:58:09	−19:10:04	3387	4	8.48	23.41	23.18	158.56	0.52	107	0.134	14	···
64	15:36:22	43:29:29	5660	5	9.62	22.19	9.19	102.35	0.71	197	0.047	28	···
65	16:12:50	33:02:06	9429	4	10.51	21.73	4.32	91.69	0.20	108	0.077	4	VV 1801
66	16:37:53	36:03:18	9614	4	9.91	22.45	7.62	105.18	0.17	204	0.047	23	···
67	19:14:47	−54:36:26	5400	4	9.48	23.15	13.64	110.24	0.13	224	0.045	33	···
68	19:51:59	−30:49:31	5891	4	9.47	20.22	3.90	46.60	0.80	368	0.011	50	HCG 86
69	20:00:59	−47:04:38	6804	4	10.02	20.19	2.92	29.28	0.16	317	0.008	30	KTS 61, Rose 38, NGC6845, VV 1880
70	20:03:14	−56:00:10	4413	4	8.01	21.62	12.97	93.18	0.30	84	0.100	3	···
71	20:17:25	−70:41:58	3969	4	7.77	22.94	28.03	167.79	0.20	488	0.031	148	VV 297
72	20:43:41	−26:34:43	12 406	4	10.45	21.45	3.81	95.20	0.68	268	0.032	38	···
73	20:47:22	00:23:32	3779	6	8.89	21.83	11.03	71.64	0.58	254	0.026	43	···
74	20:52:24	−05:45:16	6028	4	9.85	22.19	7.70	68.51	0.16	80	0.077	5	HCG 88
75	21:08:25	−29:45:32	5935	4	9.57	23.48	14.46	166.54	0.82	53	0.285	6	SCG 2105-2957
76	21:17:01	−42:19:38	5337	4	9.46	22.32	9.77	123.47	0.81	112	0.100	11	SCG 2113-4235
77	22:03:28	12:38:56	8113	4	9.83	20.15	2.66	39.48	0.51	465	0.008	69	WBL 677
78	22:36:24	−24:18:35	10 314	4	10.30	21.57	4.21	95.89	0.12	103	0.084	4	···
79	22:55:22	−33:54:22	8761	4	10.21	20.21	2.39	41.13	0.65	175	0.021	10	VV 1957
80	22:58:09	26:07:30	7588	5	9.25	22.17	8.95	137.84	0.72	201	0.062	22	UZC-CG 282, VV 84
81	23:15:18	19:00:38	4922	4	9.00	21.58	8.31	70.59	0.41	237	0.027	37	HCG 93, USGC U837, Arp 99
82	23:28:03	−67:47:18	3904	4	9.82	21.54	6.04	42.88	0.46	176	0.022	25	···
83	23:28:18	32:25:09	5066	4	9.18	21.58	7.15	68.01	0.59	344	0.018	58	···
84	23:47:27	−02:18:37	6665	5	10.07	21.38	5.23	64.89	0.73	415	0.014	94	HCG 97, RSCG 87
85	23:53:35	07:59:10	5218	5	9.15	22.68	15.93	142.35	0.52	233	0.055	33	···

Note. ID: Group ID, RA: right ascension of the CG centre, Dec.: Declination of the CG centre, v: median velocity, N: number of galaxy members in the CG in the range of 3 mag from the brightest member, K_b: Galactic extinction-corrected K-band apparent magnitude of the brightest galaxy, μ_K: Galactic extinction-corrected K-band group surface brightness, θ_G: angular diameter of the smallest circumscribed circle, $\langle R_{ij}\rangle$: median projected separation among galaxies, b/a: apparent group elongation, σ_v: radial velocity dispersion of the galaxies in the CG computed using individual galaxy errors, $H_0\,t_{cr}$: dimensionless crossing time, M_{VT}/L_K: mass-to-light ratio in the K band, cross-ID: cross-identification with other group catalogues
References for cross-ID: AM: Arp+Madore Southern Peculiar Galaxies and Associations (Arp & Madore 1987); Arp: Arp Peculiar Galaxies (Arp 1966); HCG: Hickson Compact Group (Hickson 1982); HDCE: high-density-contrast groups – erratum version (Crook et al. 2008); KPG: Karachentsev Isolated Pairs of Galaxies Catalogue (Karachentsev 1972); KTG: Karachentsev Isolated Triplets of Galaxies Catalogue (Karachentsev, Karachentsev & Lebedev 1988); KTS: Karachentseva Triple System (Karachentseva & Karachentsev 2000); M60: Mamon (1989, 2008); Rose: Rose Compact Groups of Galaxies (Rose 1977); RSCG: Redshift Survey Compact Group (Barton et al. 1996); SCG: Southern Compact Group (Prandoni et al. 1994; Iovino 2002); UZC-CG:Updated Zwicky Catalogue-Compact Group (Focardi & Kelm 2002); USGC: UZC/SSRS2 Group Catalogue (Ramella et al. 2002); VV: Interacting galaxies catalogue (Vorontsov-Velyaminov, Noskova & Arkhipova 2001) WBL: White+Bliton+Bhavsar groups (White et al. 1999).

Table C2. Table of galaxy members (*v2MCG*s). We included here only a few lines. The complete table can be found as Supporting Information with the electronic version of the article.

GroupID	GalID	RA (J2000)	Dec. (J2000)	K	k_K	v_r (km s^{-1})	err(v) (km s^{-1})	v_r Source	SDSS_ID	2MASS_ID
1	1	00:00:46.97	28:24:07.28	10.41	−0.06	8764	19	1	758874298530726152	00004696+2824071
1	2	00:00:37.94	28:23:04.34	10.46	−0.05	8705	9	1	758874298530726255	00003794+2823041
1	3	00:00:44.00	28:24:05.22	11.53	−0.04	8156	0	1	758874298530726153	00004401+2824051
1	4	00:00:42.41	28:22:08.43	13.26	−0.03	9006	0	2	758874298530791466	00004242+2822081
1	5	00:00:45.09	28:22:18.18	13.40	−0.08	8642	0	2	758874298530791773	00004507+2822181
2	1	00:01:02.89	−43:19:49.57	10.14	−0.07	11627	45	1	000000000000000000	00010289–4319496
2	2	00:00:53.00	−43:23:31.43	11.59	−0.05	11980	40	1	000000000000000000	00005298–4323316
2	3	00:00:57.05	−43:25:47.60	12.27	−0.06	10964	45	2	000000000000000000	00005702–4325476
2	4	00:00:52.18	−43:20:02.38	12.47	−0.06	11422	0	2	000000000000000000	00005216–4320026

Note. Group ID, Galaxy ID, RA: right ascension, Dec.: declination, K: Galactic extinction-corrected K-band apparent magnitude, k_K k-correction in the K band computed from Chilingarian et al. (2010) as a function of redshift and colour $H-K$, v_r: radial velocity, err$_{v_r}$: error in radial velocity, v_r_source: catalogue from which the v_r and err$_{v_r}$ were extracted, SDSS_ID: ObjectID in the SDSS DR7 data base, 2MASS_ID: ID in the 2MASS data base.
References for redshift source:
1 = main 2MRS (Huchra et al. 2012).
2 = extra 2MRS (Huchra et al. 2012).
3 = 2M++ redshift catalogue (Lavaux & Hudson 2011).
0 = NED.

SUPPORTING INFORMATION

Additional Supporting Information may be found in the online version of this article:

Table C2. Table of galaxy members in compact groups identified from the 2MASS catalogue (v2MCGs).

Please note: Wiley-Blackwell are not responsible for the content or functionality of any supporting materials supplied by the authors. Any queries (other than missing material) should be directed to the corresponding author for the article.

This paper has been typeset from a TEX/LATEX file prepared by the author.